Photoionized Plasmas: Connections Between Laboratory and Astrophysical Plasmas

David Cohen
Swarthmore College

Collaboration with R. Mancini, J. Bailey, G. Rochau

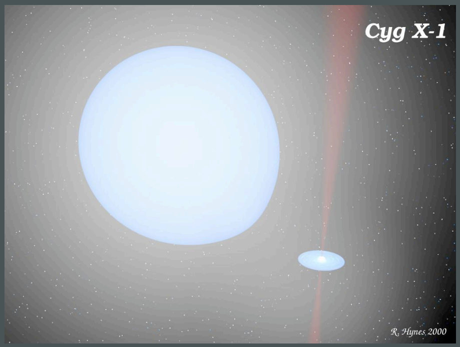

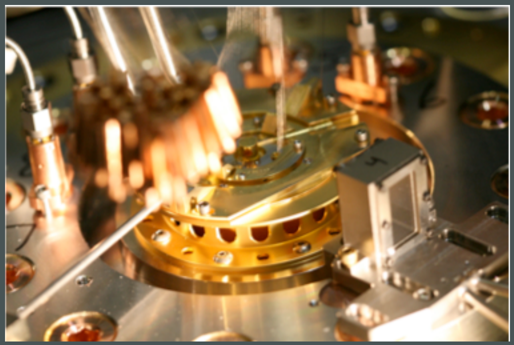

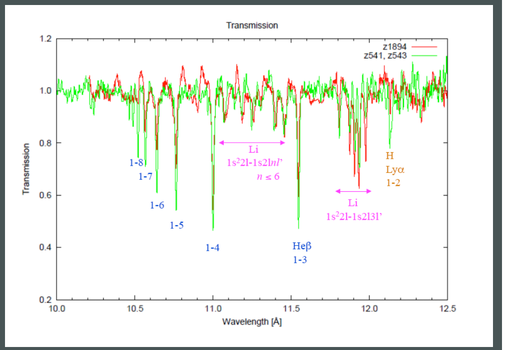

My background/perspective:

Traditional astrophysicist (massive stars, their winds, and x-ray emission)

At an undergraduate-only college (1500 students in total; 15 physics majors per class year; >50% to PhD programs)

(I have done some work in ICF and lab astro, too)

Small liberal arts colleges disproportionately produce students who go on to earn physics PhDs

e.g. Bill Goldstein, John Mather are Swarthmore College alumni

My own students:

Amy Reighard (2001) – Michigan – LLNL
Vernon Chaplin (2007) – Caltech
Mike Rosenberg (2008) – MIT

We study black holes (and neutron stars) by watching material fall onto them

Hard x-rays from accretion photoionize surrounding (accreting) material – we need to interpret the spectra

Broad (astro) science goals:

- Compact object and accretion physics
- Physical conditions in the stellar winds/mass-flows
- Stellar evolution and populations
- Astrophysical jets
- Galactic structure
- Effect of super-massive black hole “feedback” on large scale structure formation

Large Scale Structure of the Universe:

Gravity from dark matter

And

Energy injection from AGN ("feedback")

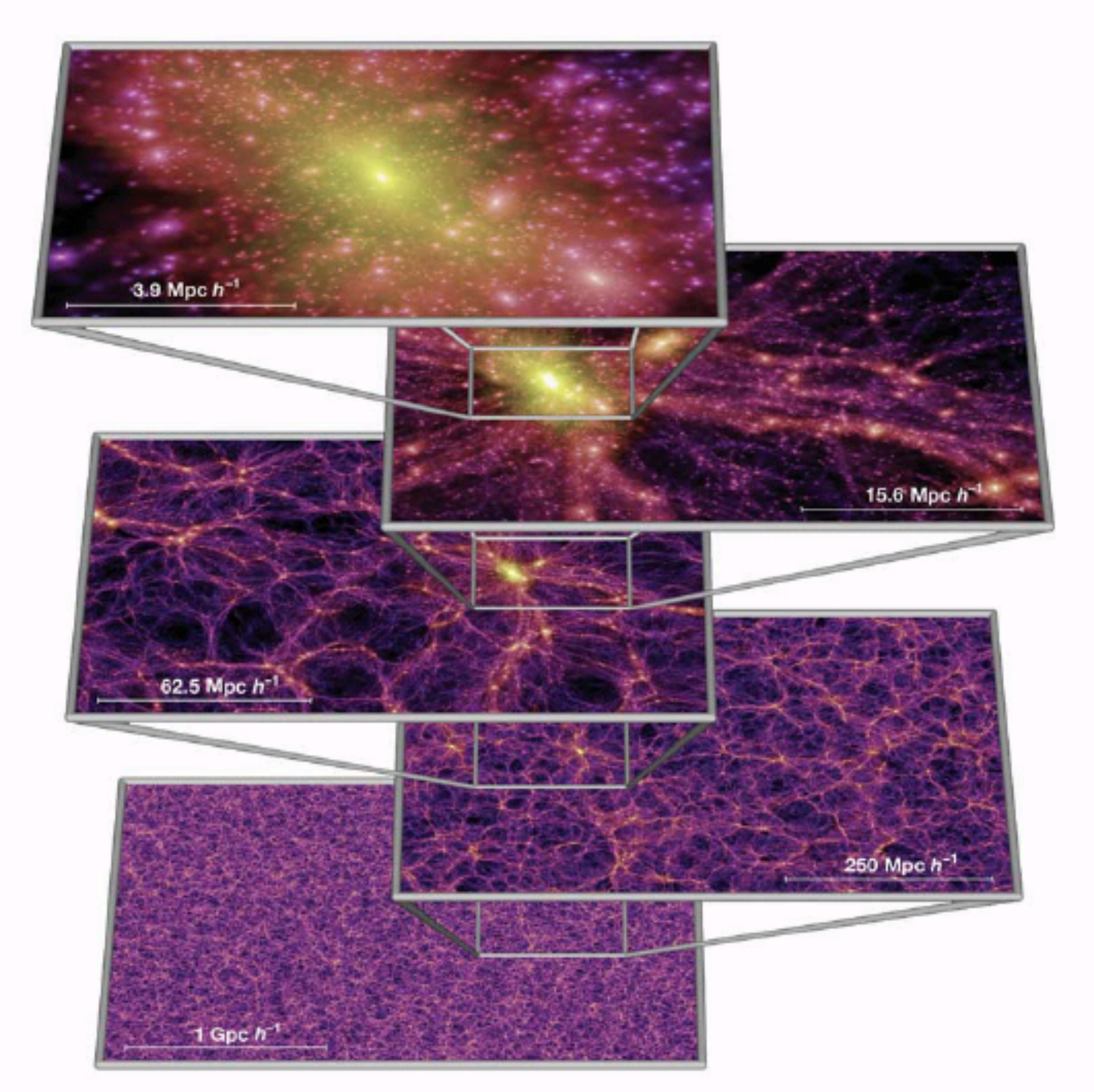

Millennium simulation

High-Mass X-ray Binary (HMXRB): Direct wind accretion onto a stellar mass compact object

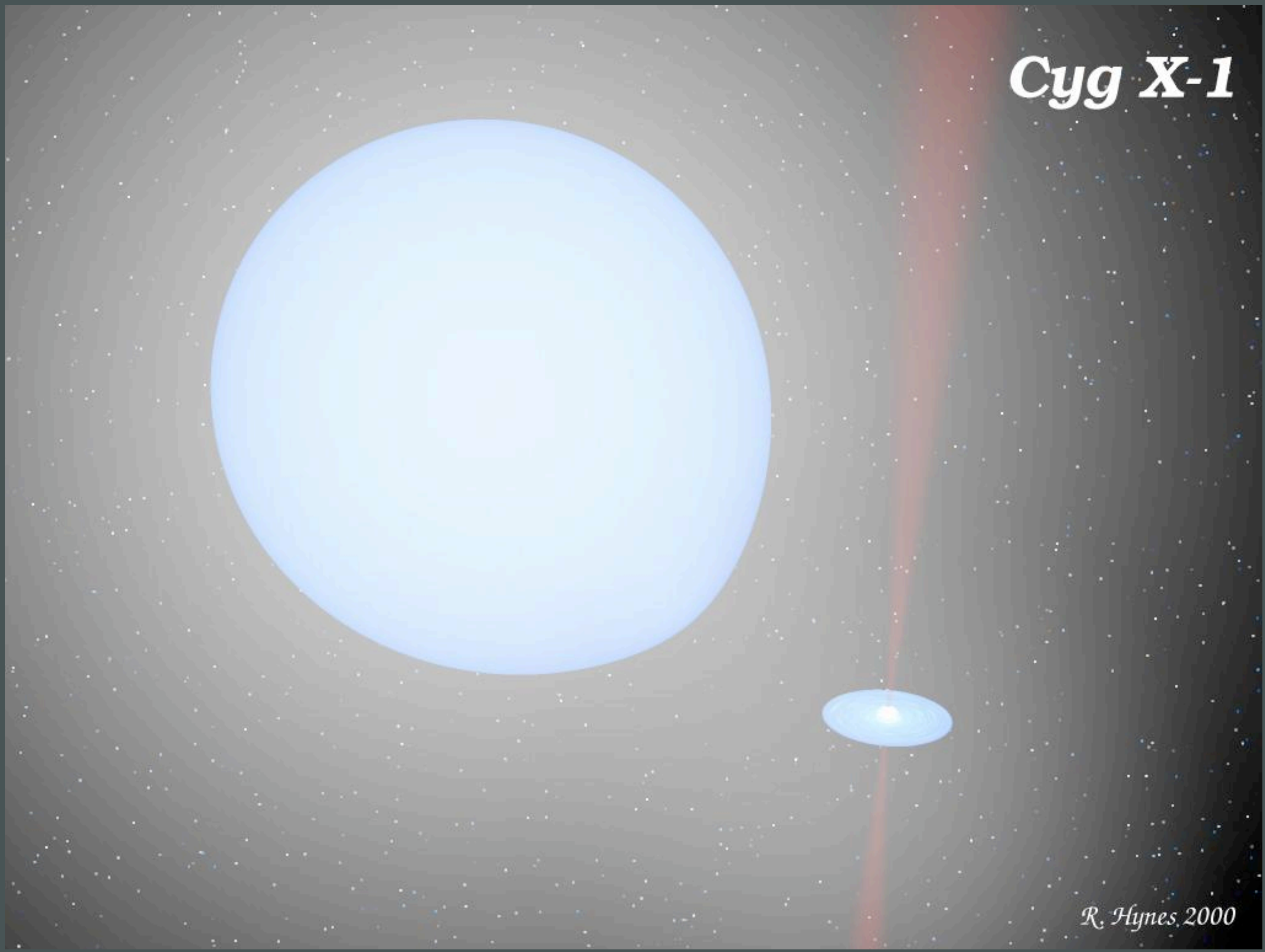

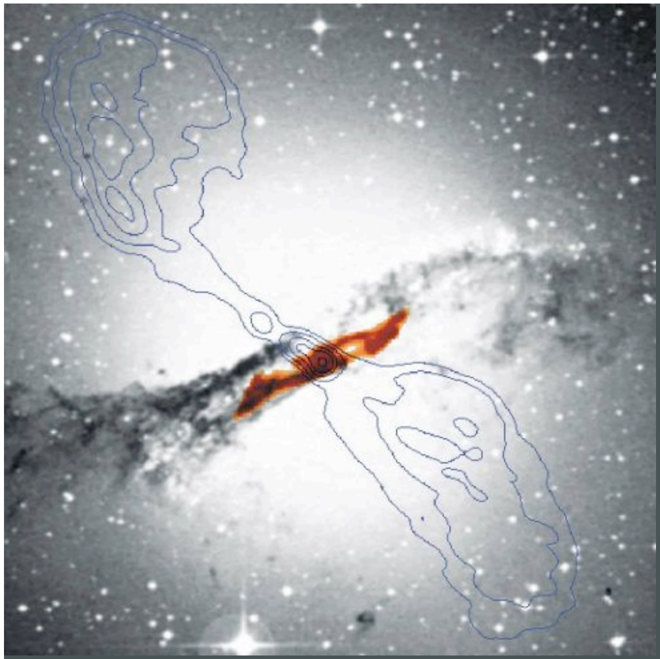

Active Galactic Nucleus (AGN): accretion onto a ~10^9 M_{sun} black hole

M 82 – red is X-ray emission

THE ASTROPHYSICAL JOURNAL, **350**: L37–L40, 1990 February 20

X-RAY SPECTRAL SIGNATURES OF PHOTOIONIZED PLASMAS

DUANE A. LIEDAHL AND STEVEN M. KAHN
Department of Physics and Space Sciences Laboratory, University of California, Berkeley

AND

ALBERT L. OSTERHELD AND WILLIAM H. GOLDSTEIN
Lawrence Livermore National Laboratory
Received 1989 September 13; accepted 1989 December 1

ABSTRACT

Plasma emission codes have become a standard tool for the analysis of spectroscopic data from cosmic X-ray sources. However, the assumption of collisional equilibrium, typically invoked in these codes, renders them inapplicable to many important astrophysical situations, particularly those involving X-ray photoionized nebulae. We illustrate this point by comparing model spectra which have been calculated under conditions appropriate to both coronal plasmas and X-ray photoionized plasmas. We show that the $(3s–2p)/(3d–2p)$ line ratios in the Fe L-shell spectrum can be used to effectively discriminate between these two cases. This diagnostic will be especially useful for data analysis associated with *AXAF* and *XMM*, which will carry spectroscopic instrumentation with sufficient sensitivity and resolution to identify X-ray photoionized nebulae in a wide range of astrophysical environments.

Subject headings: atomic processes — line formation — X-rays: binaries — X-rays: spectra

Iron models with same ionization balance – very different emission properties (coronal: left and photoionized: right)

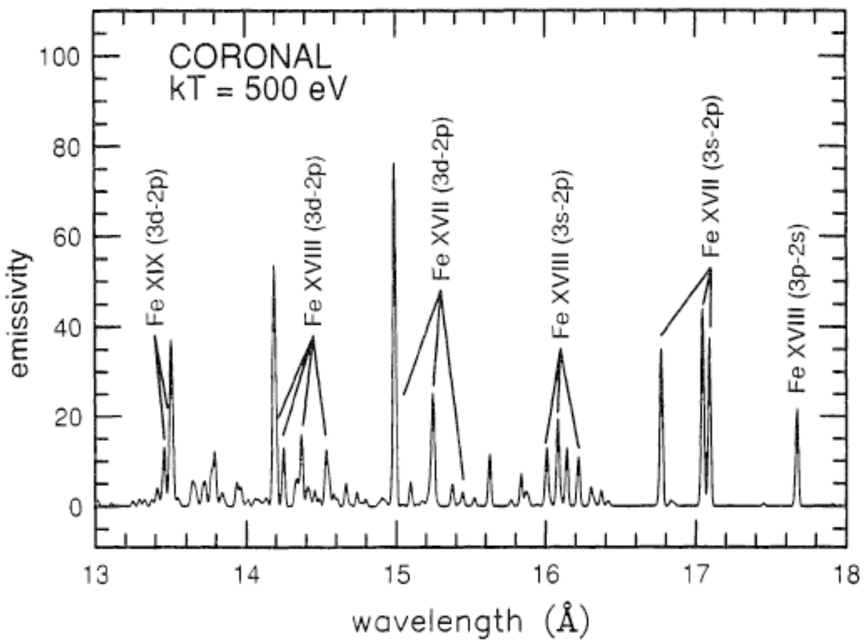

FIG. 1.—Model emission rate spectrum for Fe XVI–XIX under conditions appropriate to coronal equilibrium, $kT_e = 500$ eV, $n_e = 10^{11}$ cm^{-3}. The line profiles are Gaussian with a FWHM of 0.025 Å. The emissivity scale is arbitrary.

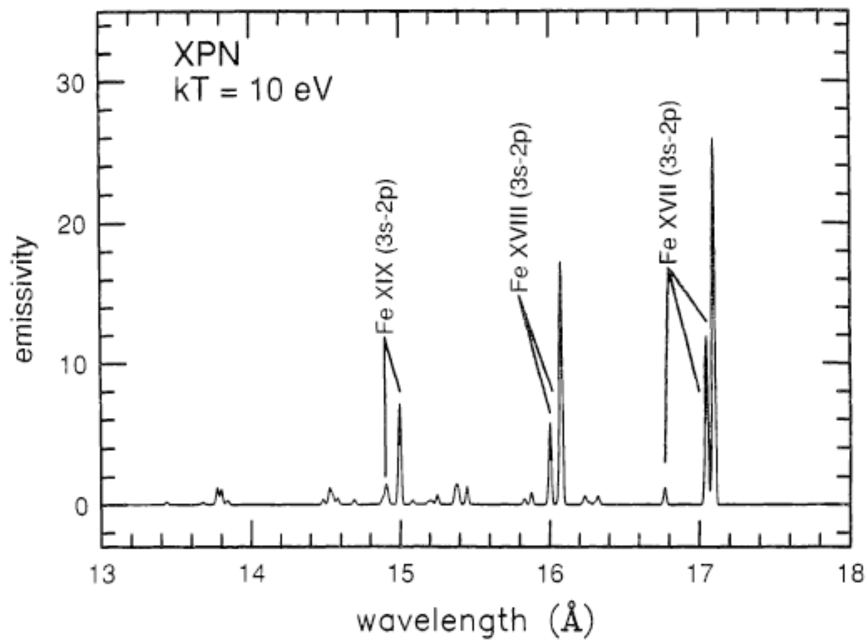

FIG. 2.—Model emission rate spectrum for Fe XVII–XIX under conditions appropriate to an X-ray–photoionized nebula, $kT_e = 10$ eV, $n_e = 10^{11}$ cm^{-3}. The line profiles and emissivity scale are the same as for Fig. 1.

THE ASTROPHYSICAL JOURNAL, 525:921–934, 1999 November 10

THE X-RAY SPECTRUM AND GLOBAL STRUCTURE OF THE STELLAR WIND IN VELA X-1

MASAO SAKO,[1] DUANE A. LIEDAHL,[2] STEVEN M. KAHN,[1] AND FRITS PAERELS[1,3]
Received 1999 January 28; accepted 1999 July 2

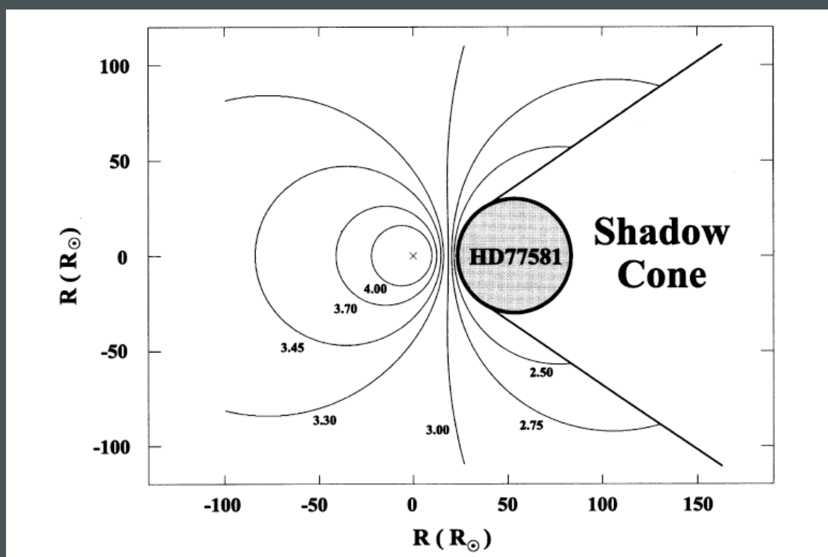

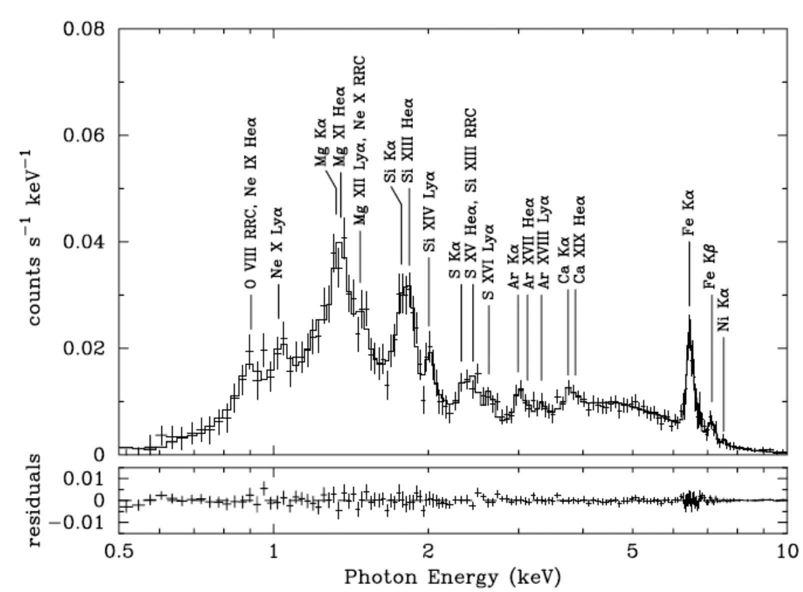

FIG. 1.—*ASCA* SIS0 data and the best-fit recombination cascade model. The strongest recombination and fluorescent lines are labeled. SIS1 data was also used in the analysis but are not shown for clarity.

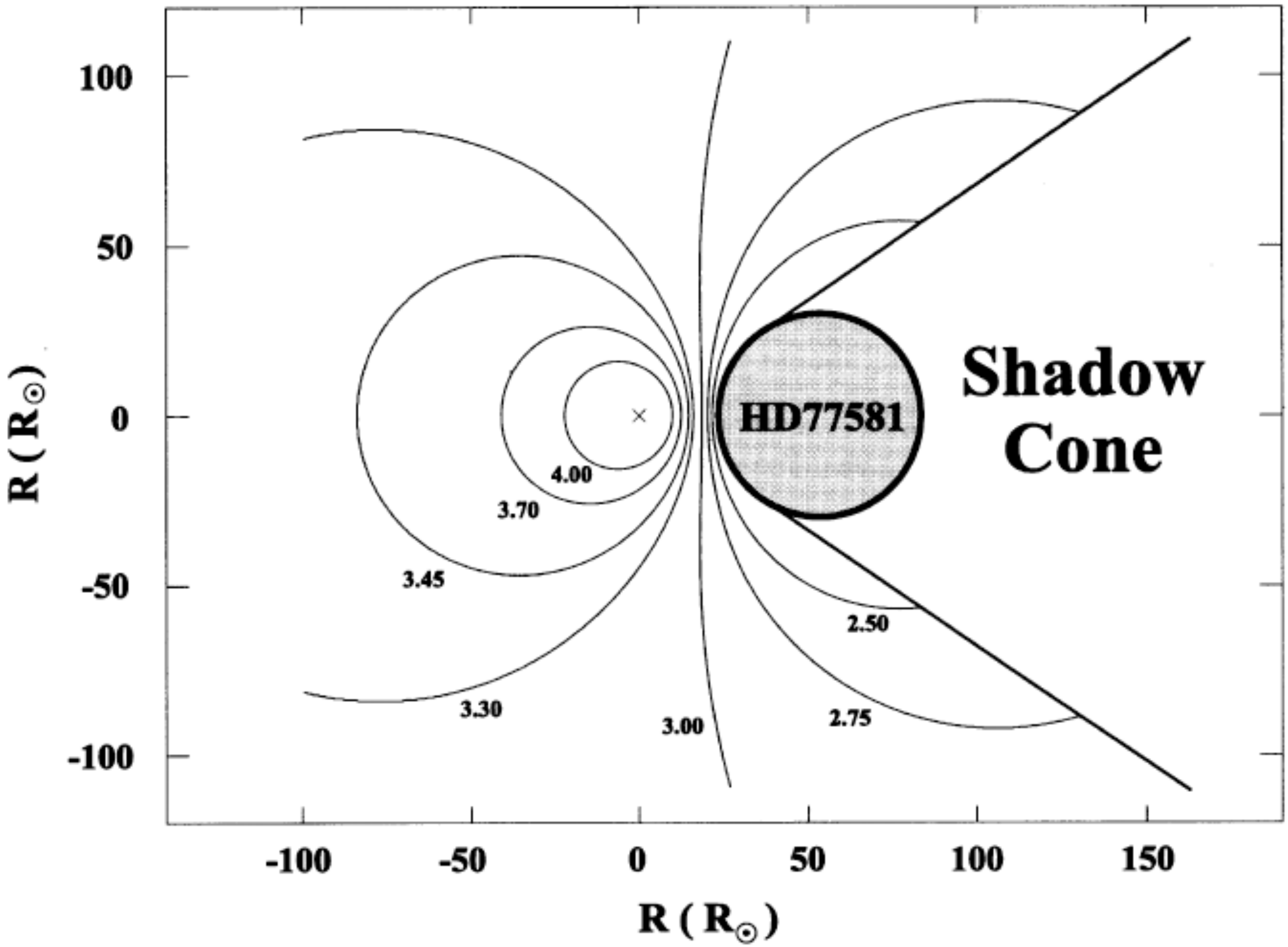

Shadow
Cone
HD77581
4.00
3.70
3.45
3.30
3.00
2.50
2.75
100
50
0
-50
-100
150
R ($R_\odot$)
R ($R_\odot$)

Ionization parameter – describes physical conditions

$$\xi = L/r^2 n \text{ (ergs cm s}^{-1}\text{)}$$

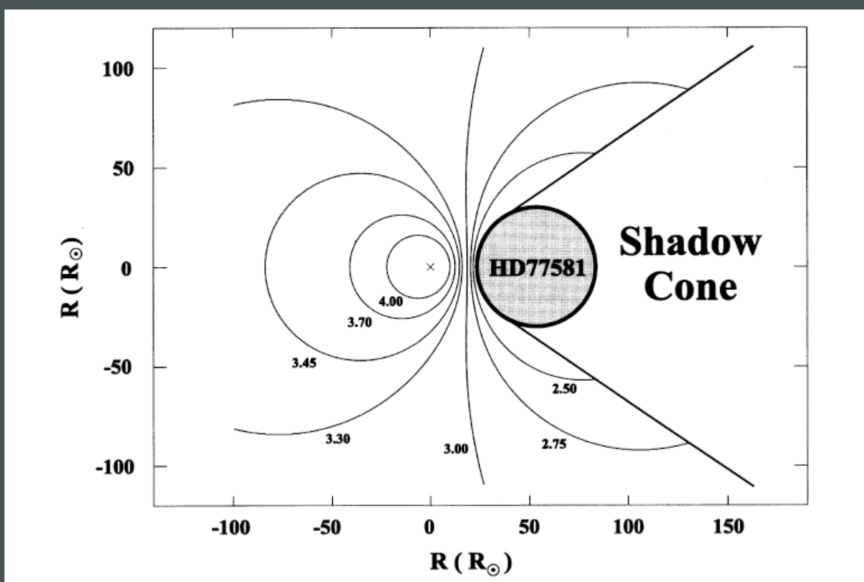

Ranges from 100 to 10,000 (cgs units)

ASCA (Japan) – state of the art 1999

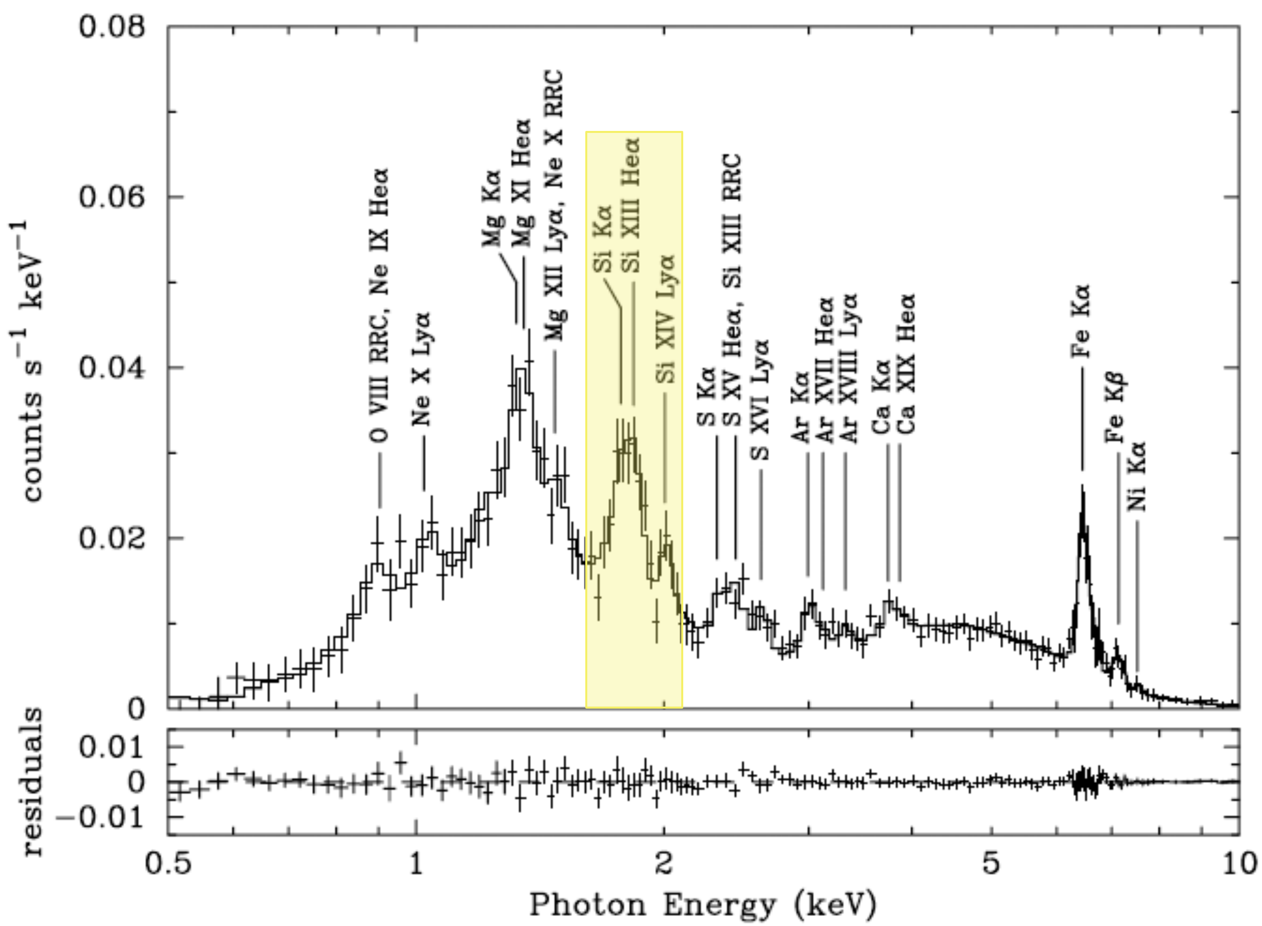

FIG. 1.—*ASCA* SIS0 data and the best-fit recombination cascade model. The strongest recombination and fluorescent lines are labeled. SIS1 data was also used in the analysis but are not shown for clarity.

Distribution of plasma vs. ionization parameter

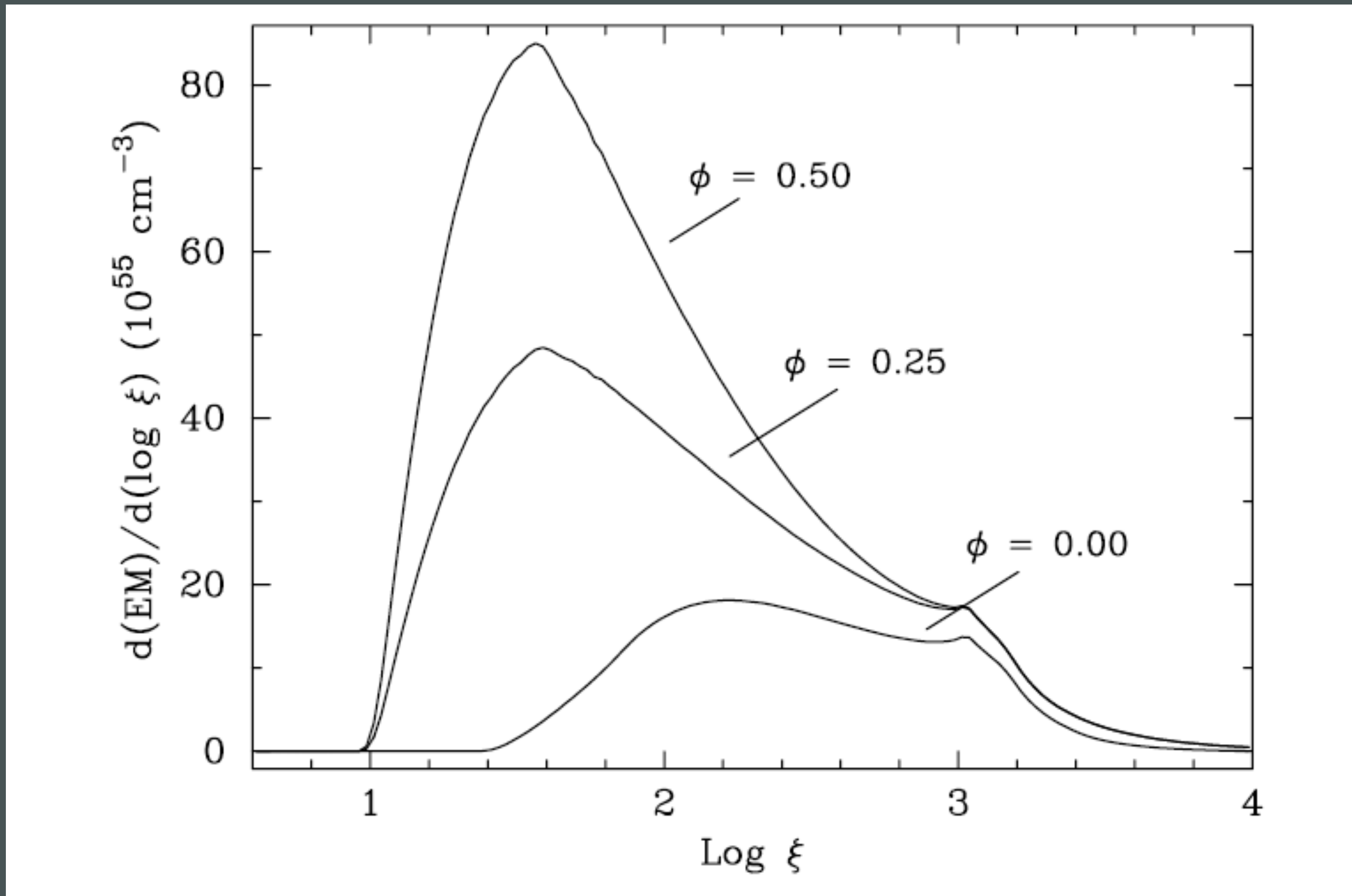

Peak at low values indicates high-density clumps

The Astrophysical Journal, 651:421–437, 2006 November 1

X-RAY SPECTRAL STUDY OF THE PHOTOIONIZED STELLAR WIND IN VELA X-1

Shin Watanabe,[1] Masao Sako,[2] Manabu Ishida,[3] Yoshitaka Ishisaki,[3] Steven M. Kahn,[2] Takayoshi Kohmura,[4]
Fumiaki Nagase,[1] Frederik Paerels,[5] and Tadayuki Takahashi[1]
Received 2006 February 15; accepted 2006 July 1

ABSTRACT

We present results from quantitative modeling and spectral analysis of the high-mass X-ray binary system Vela X-1 obtained with the *Chandra* HETGS. The spectra exhibit emission lines from H- and He-like ions driven by photoionization, as well as fluorescent emission lines from several elements in lower charge states. The properties of these X-ray lines are measured with the highest accuracy to date. In order to interpret and make full use of the data, we have developed a simulator, which calculates the ionization structure of a stellar wind and performs Monte Carlo simulations of X-ray photons propagating through the wind. From comparisons of the observed spectra with results from the simulator, we are able to find the ionization structure and the geometrical distribution of material in the stellar wind that can reproduce the observed spectral line intensities and continuum shapes remarkably well. We find that the stellar wind profile can be represented by a CAK model with a star mass-loss rate of $(1.5\text{–}2.0) \times 10^{-6}\, M_{\odot}\, \mathrm{yr}^{-1}$, assuming a terminal velocity of 1100 km s^{-1}. It is found that a large fraction of emission lines from highly ionized ions are formed in the region between the neutron star and the companion star. We also find that the fluorescent lines must be produced in at least three distinct regions: the extended stellar wind, reflection off the stellar photosphere, and in a distribution of dense material partially covering and possibly trailing the neutron star, which may be associated with an accretion wake. Finally, from detailed analysis of the emission-line profiles, we demonstrate that the stellar wind dynamics is affected by X-ray photoionization.

Subject headings: stars: neutron — stars: winds, outflows — X-rays: binaries — X-rays: individual (Vela X-1)

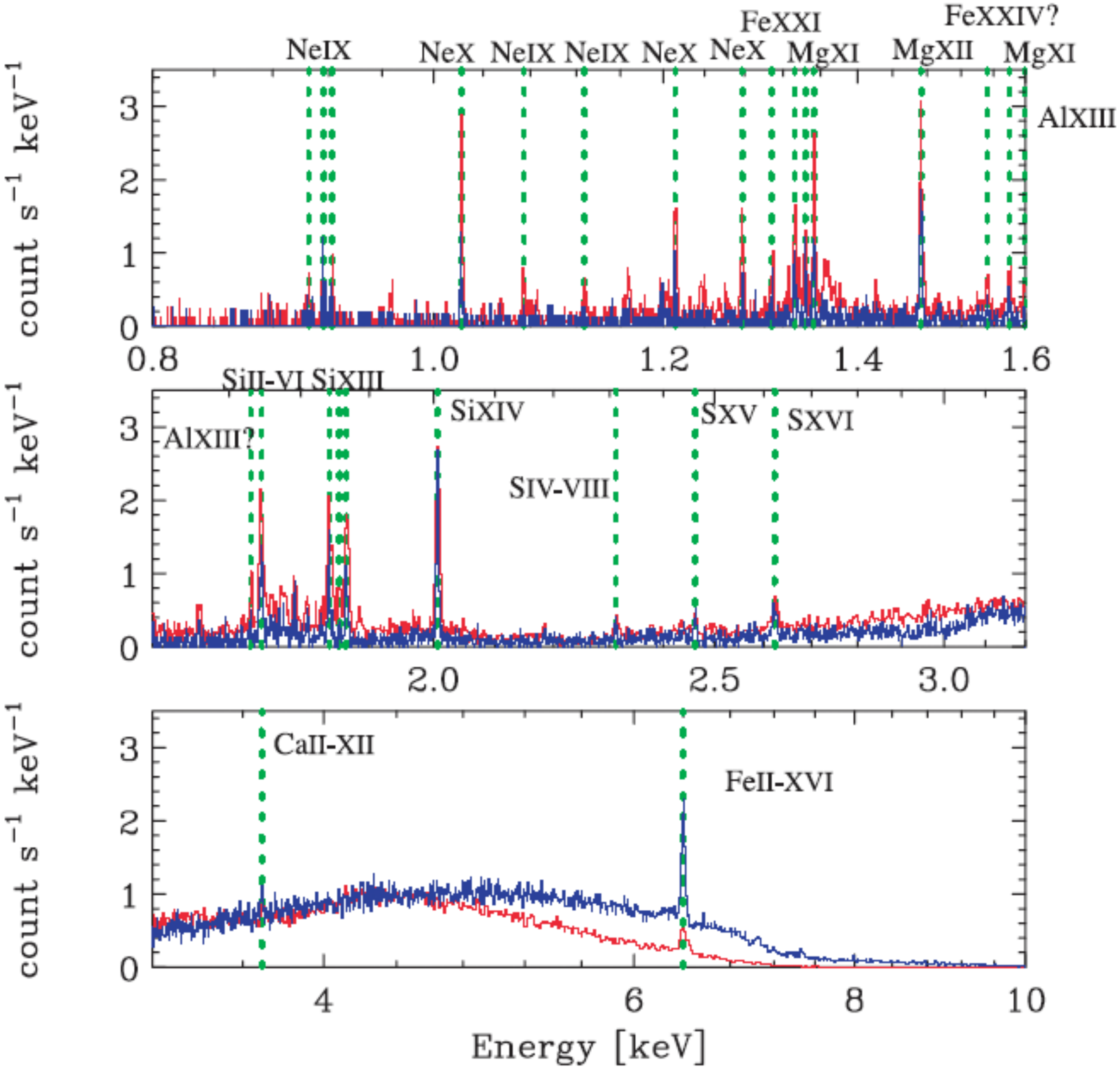

FIG. 3.—Detailed view of the Vela X-1 spectrum at phase 0.50; MEG data in red and HEG data in blue. The spectrum is dominated by discrete features below $E \sim 3$ keV. The vertical green lines label the observed emission lines that are listed in Table 3.

Chandra (US) state of the art today

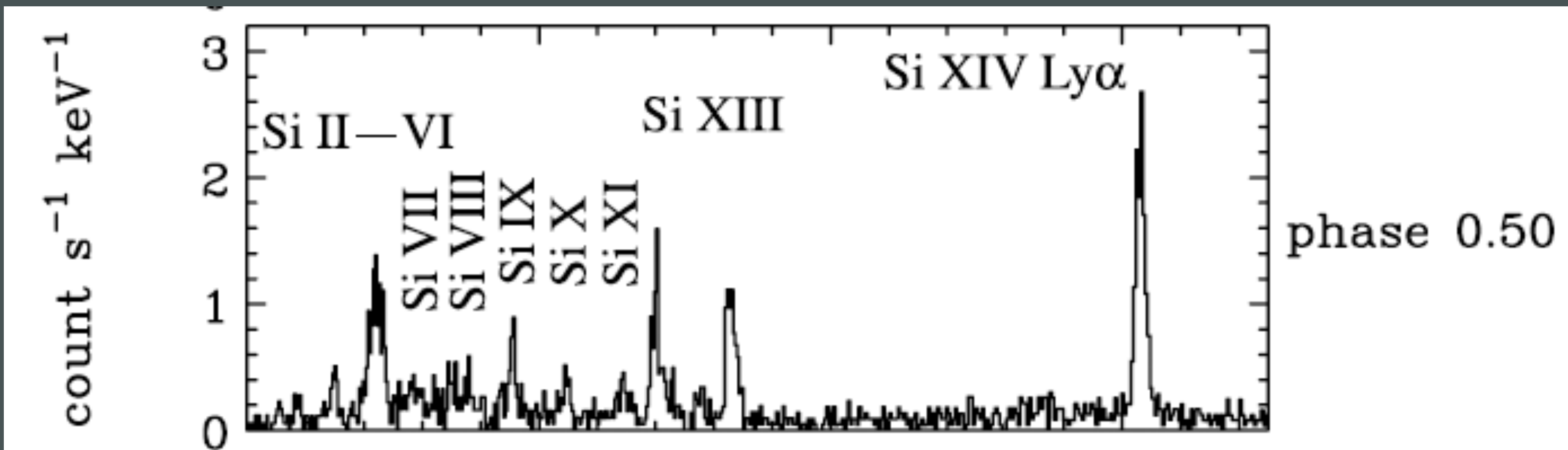

Low ionization state satellites – fluorescence in high-density clumps

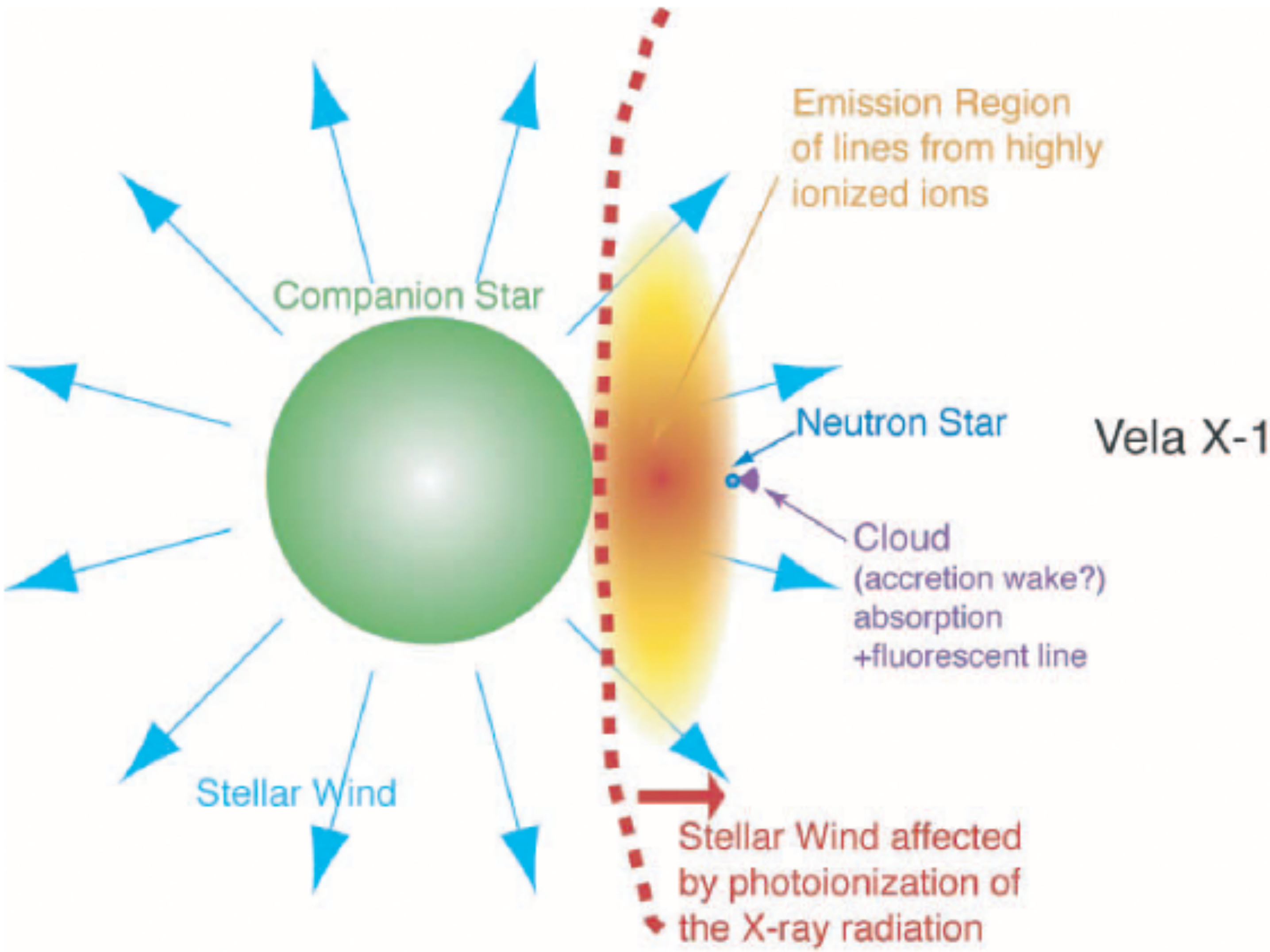

FIG. 24.—Conceptual picture of the Vela X-1 system obtained from the present analysis.

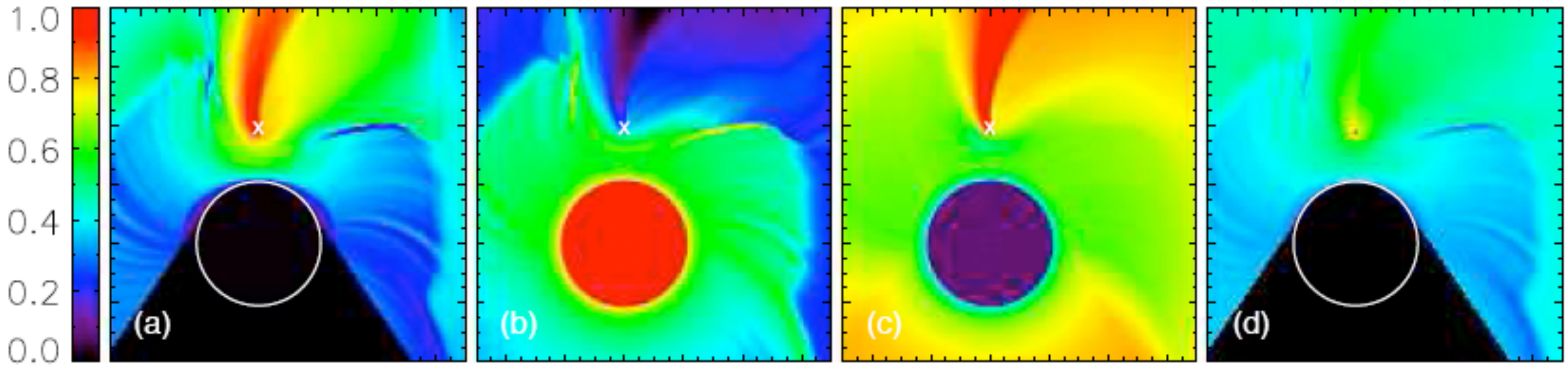

FIGURE 2. Color-coded maps of (*a*) $\log T\,(\mathrm{K}) = [4.4, 8.3]$, (*b*) $\log n\,(\mathrm{cm}^{-3}) = [7.4, 10.8]$, (*c*) $\log v\,(\mathrm{km\ s}^{-1}) = [1.3, 3.5]$, and (*d*) $\log \xi\,(\mathrm{erg\ cm\ s}^{-1}) = [1.1, 7.7]$ in the orbital plane of Vela X-1. The positions of the B star and neutron star are shown by the circle and the "×," respectively. The horizontal axis $x = [-5, 7] \times 10^{12}$ cm and the vertical axis $y = [-4, 8] \times 10^{12}$ cm.

Mauche et al. 2008, "The Physics of Wind-Fed Accretion"

DEM of ξ distribution (combined with modeling):

Wind density and inhomogeneity (clumping)
Dynamics and accretion
Ionization and feedback on the dynamics

Broadly:

How will this system evolve?

When we find other systems with quantitative differences in their x-ray spectra, what can we infer about their physical properties?

Extragalactic sources: Active Galactic Nuclei (AGN)

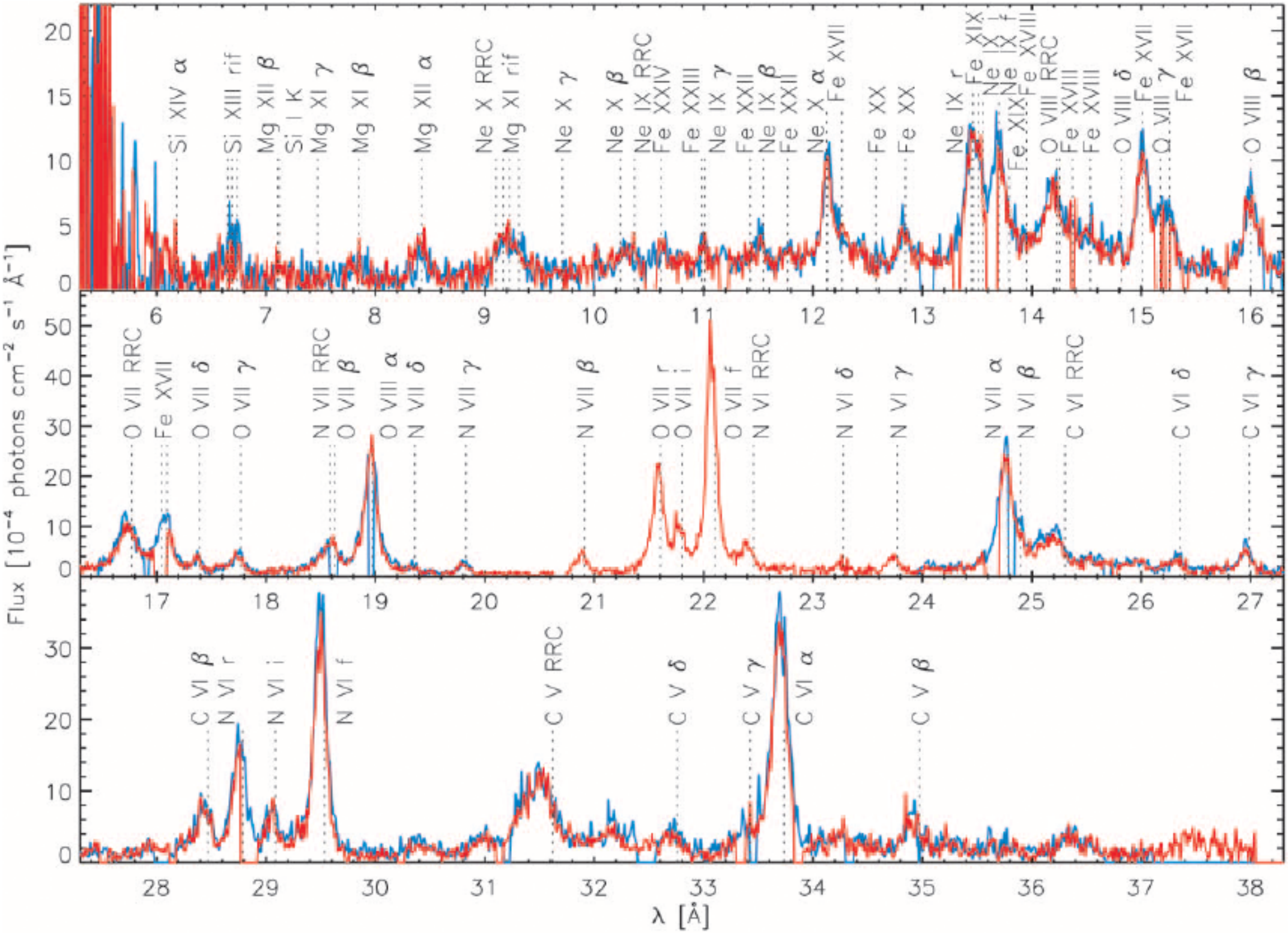

Flux [10⁻⁴ photons cm⁻² s⁻¹ Å⁻¹]
λ [Å]
Si XIV α
Si XIII rif
Mg XII β
Si I K
Mg XI γ
Mg XI β
Mg XII α
Ne X RRC
Mg XI rif
Ne X γ
Ne X β
Ne IX RRC
Fe XXIV
Fe XXIII
Ne IX γ
Fe XXII
Ne IX β
Fe XXII
Ne X α
Fe XVII
Fe XX
Fe XX
Ne IX r
Fe XIX
Ne IX i
Ne IX f
Fe XIX
Fe XVIII
O VIII RRC
Fe XVIII
Fe XVIII
O VIII δ
Fe XVII
O VIII γ
Fe XVII
O VIII β
O VII RRC
Fe XVII
O VII δ
O VII γ
N VII RRC
O VII β
O VIII α
N VII δ
N VII γ
N VII β
O VII r
O VII i
O VII f
N VI RRC
N VI δ
N VI γ
N VII α
N VI β
C VI RRC
C VI δ
C VI γ
C VI β
N VI r
N VI i
N VI f
C V RRC
C V δ
C V γ
C VI α
C V β

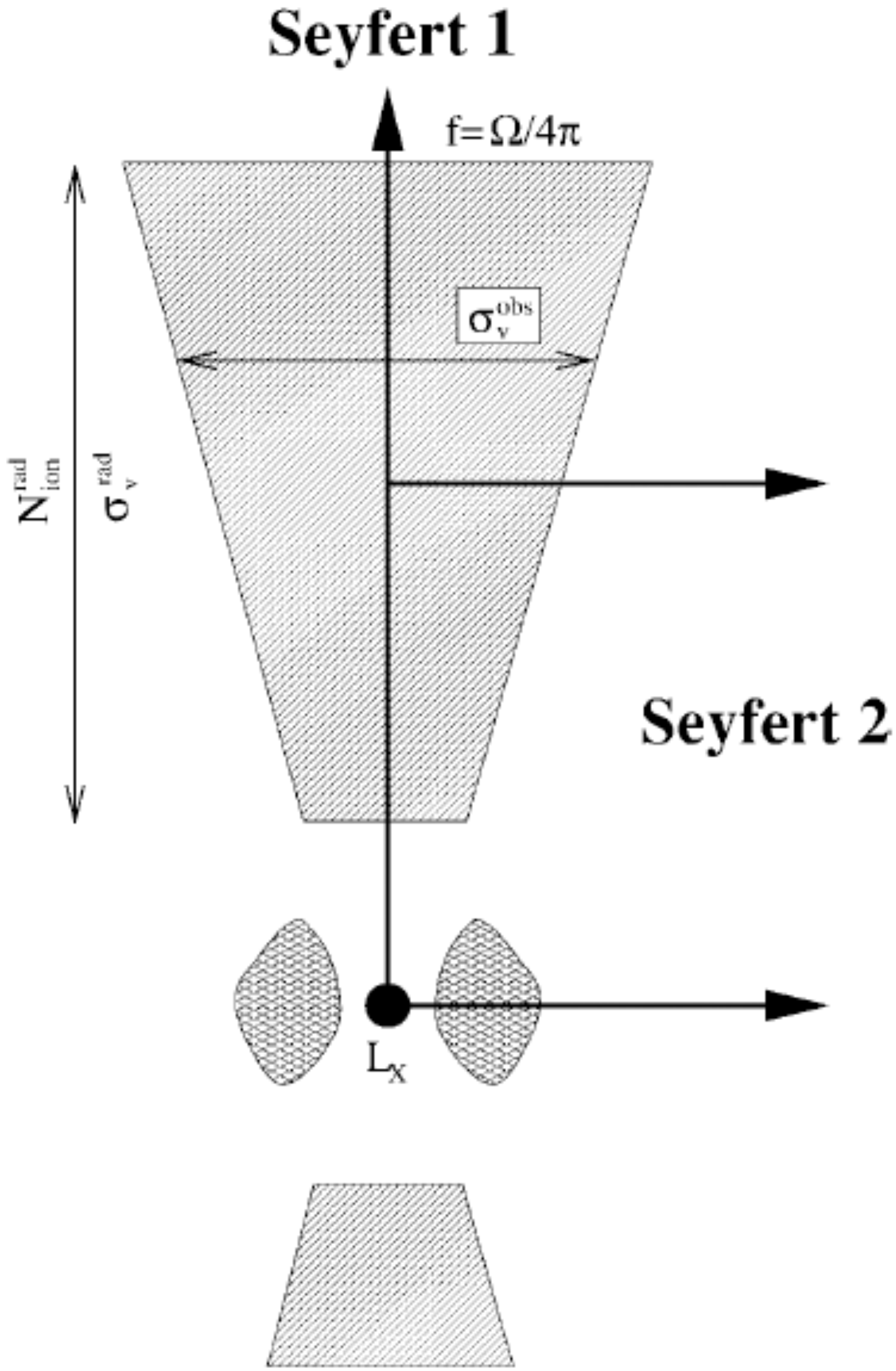
Seyfert 1
$f=\Omega/4\pi$
σ_v^{obs}
N_{ion}^{rad}
σ_v^{rad}
Seyfert 2
L_X

Challenges

Scaling – e.g. in photoionized sources:

- Low densities (else collisional); but then equilibration?
- Significant optical depths (else RT effects not accounted for)
- Thus, large linear scales – incompatible with the lab

Challenges

Systems are integrated:

- Gravity
- Hydro
- Atomic physics
- Excitation/ionization kinetics
- Radiation transport

Obvious astrophysical relevance is easiest to realize and demonstrate when:

- Measurements are local
- Small subset of an integrated problem is probed

Photoionization experiments on the Z-Machine

Side, cm-scale gas cells have been fielded at Z

10^{18} cm^{-3} of neon

- Photoionized plasma experiments are performed as "ride-along" in Z opacity shots
- Gas cell targets were designed at Sandia and fabricated in the UNR Physics machine shop

Two-window gas cell

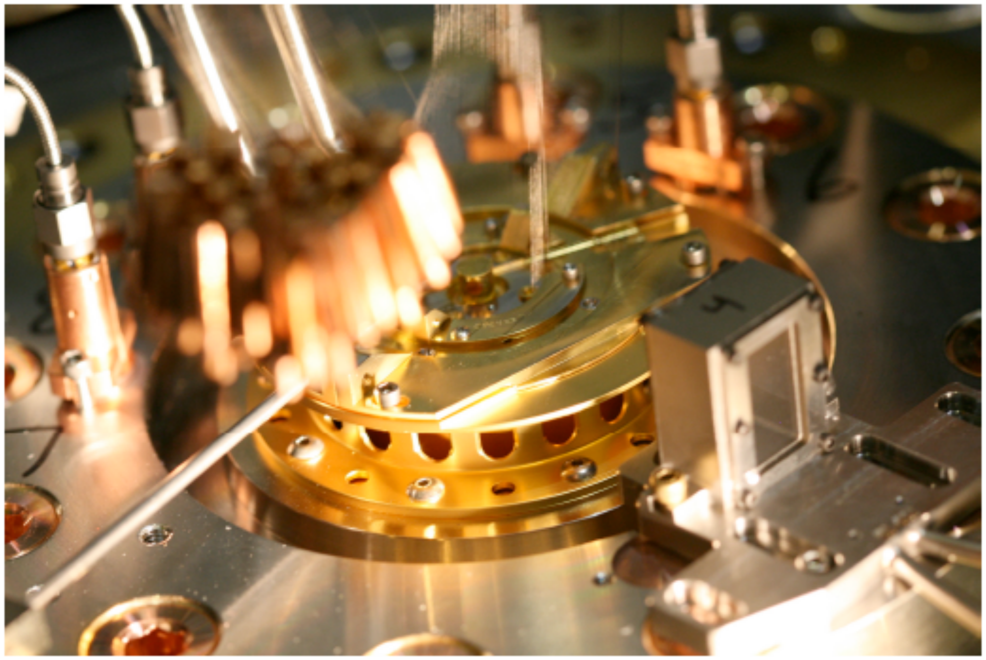

Four-window gas cell

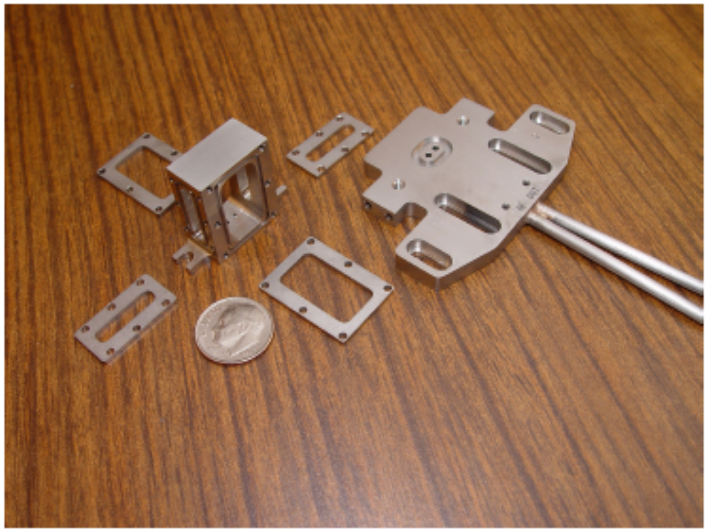

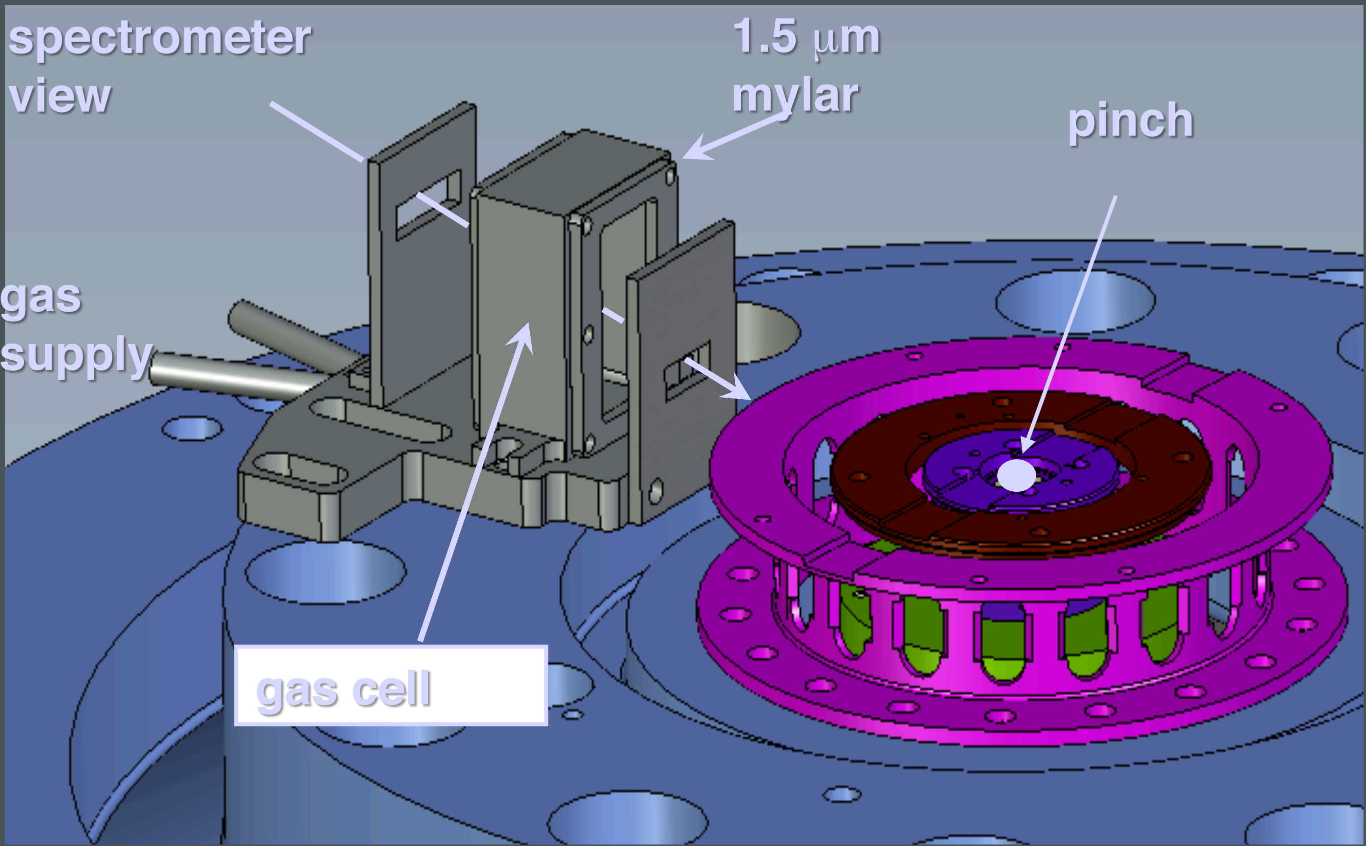
spectrometer
view
1.5 μm
mylar
pinch
gas
supply
gas cell

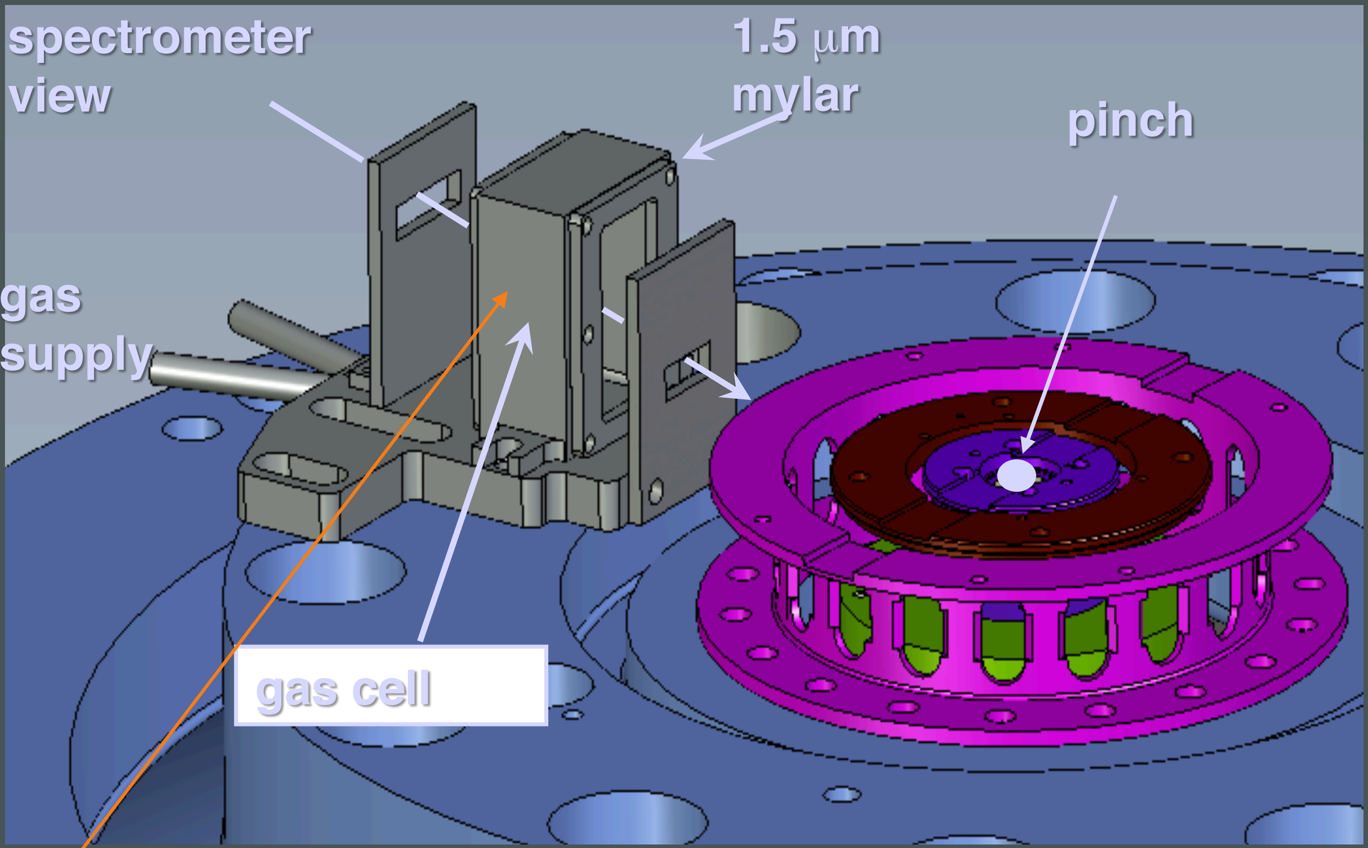

Side view with second spectrometer – measure recombination spectrum

View-factor (VisRad: Prism) model (MacFarlane et al.) constructed by Swarthmore undergraduate, M. Rosenberg

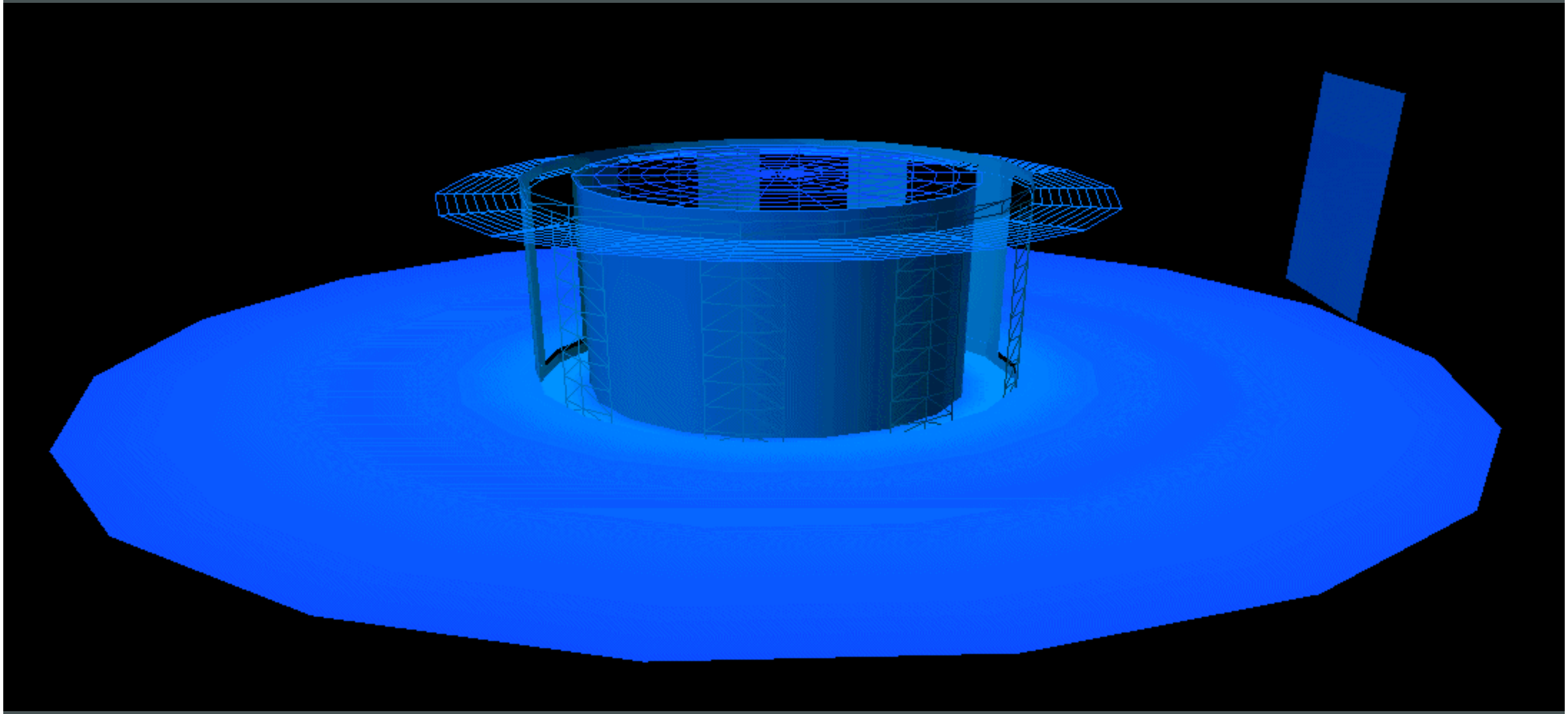

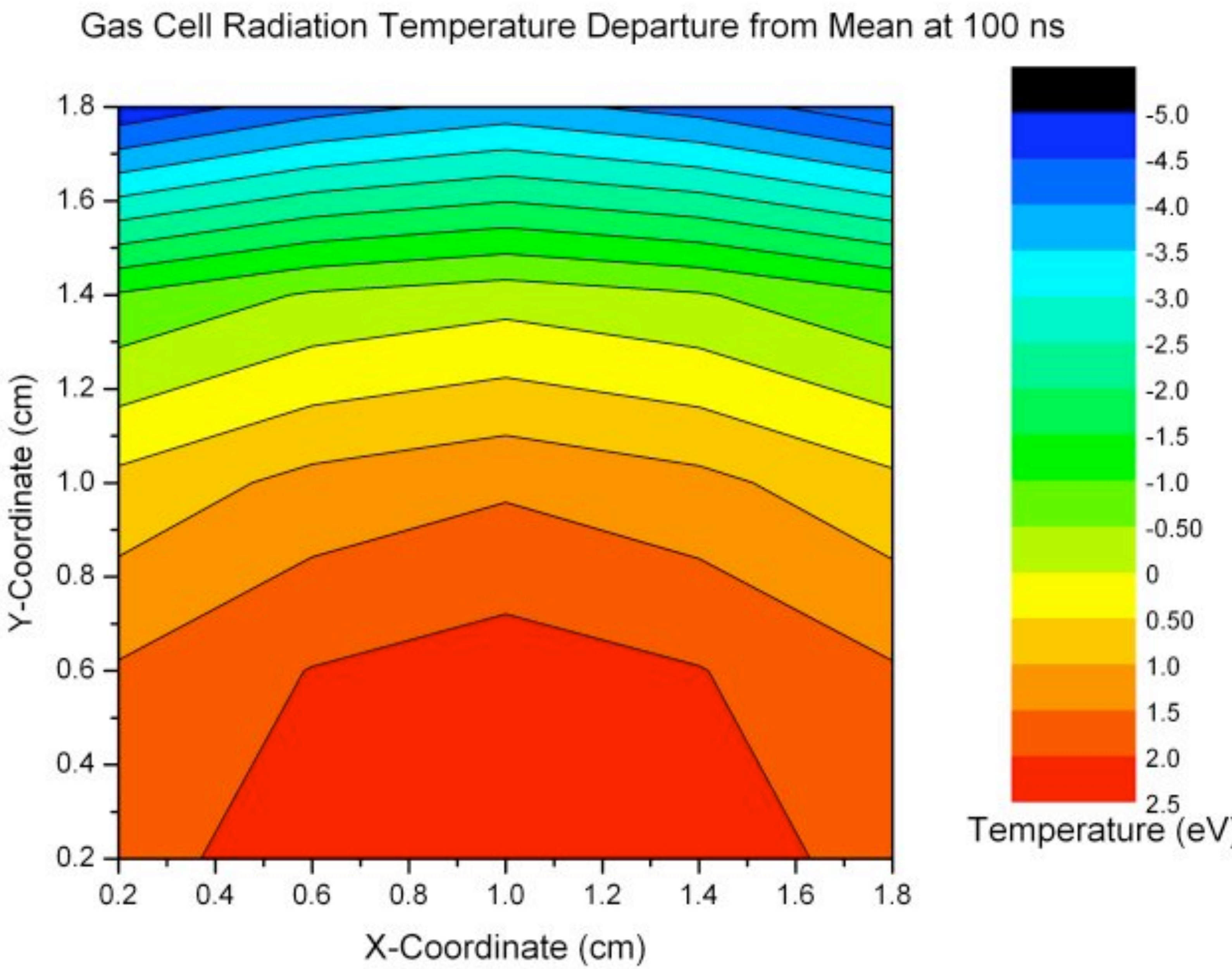
Gas Cell Radiation Temperature Departure from Mean at 100 ns
Y-Coordinate (cm)
X-Coordinate (cm)
0.2
0.4
0.6
0.8
1.0
1.2
1.4
1.6
1.8
-5.0
-4.5
-4.0
-3.5
-3.0
-2.5
-2.0
-1.5
-1.0
-0.50
0
0.50
1.0
1.5
2.0
2.5
Temperature (eV)

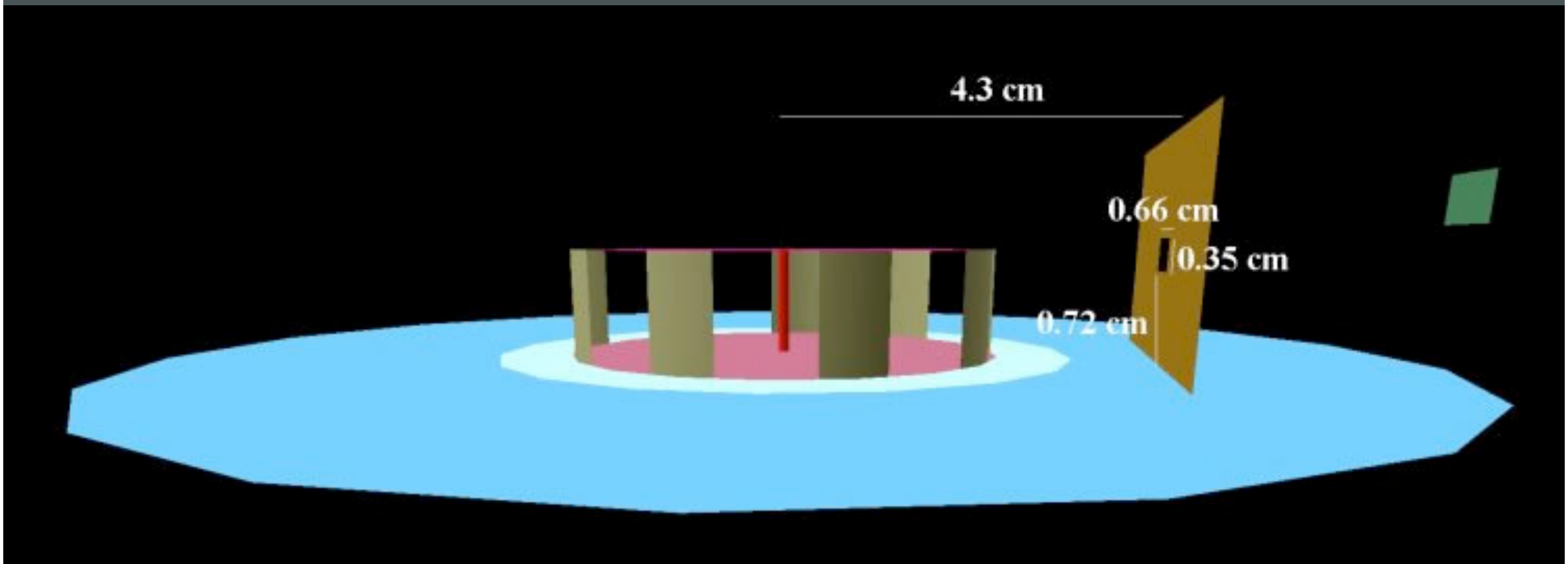
4.3 cm
0.66 cm
0.35 cm
0.72 cm

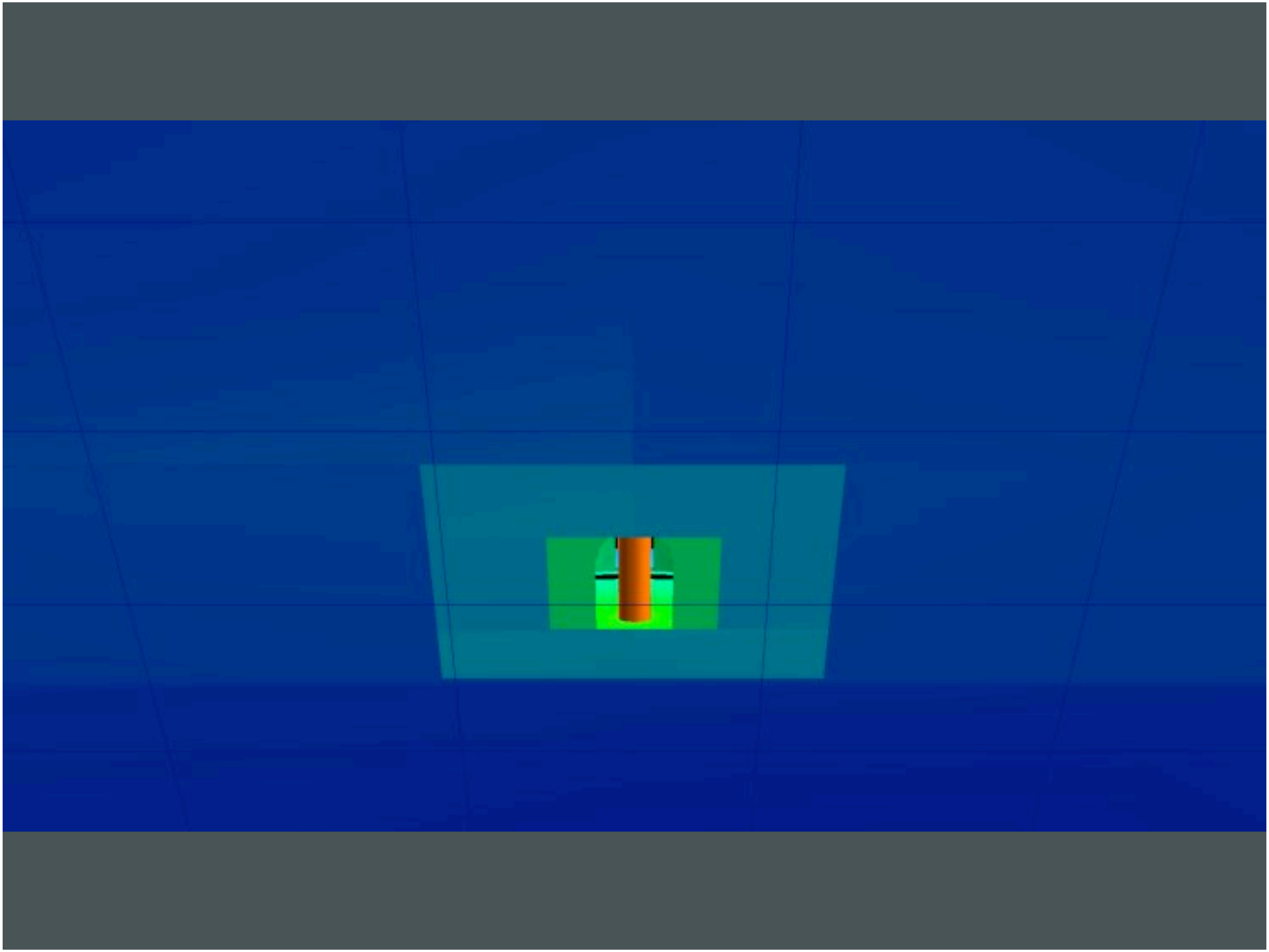

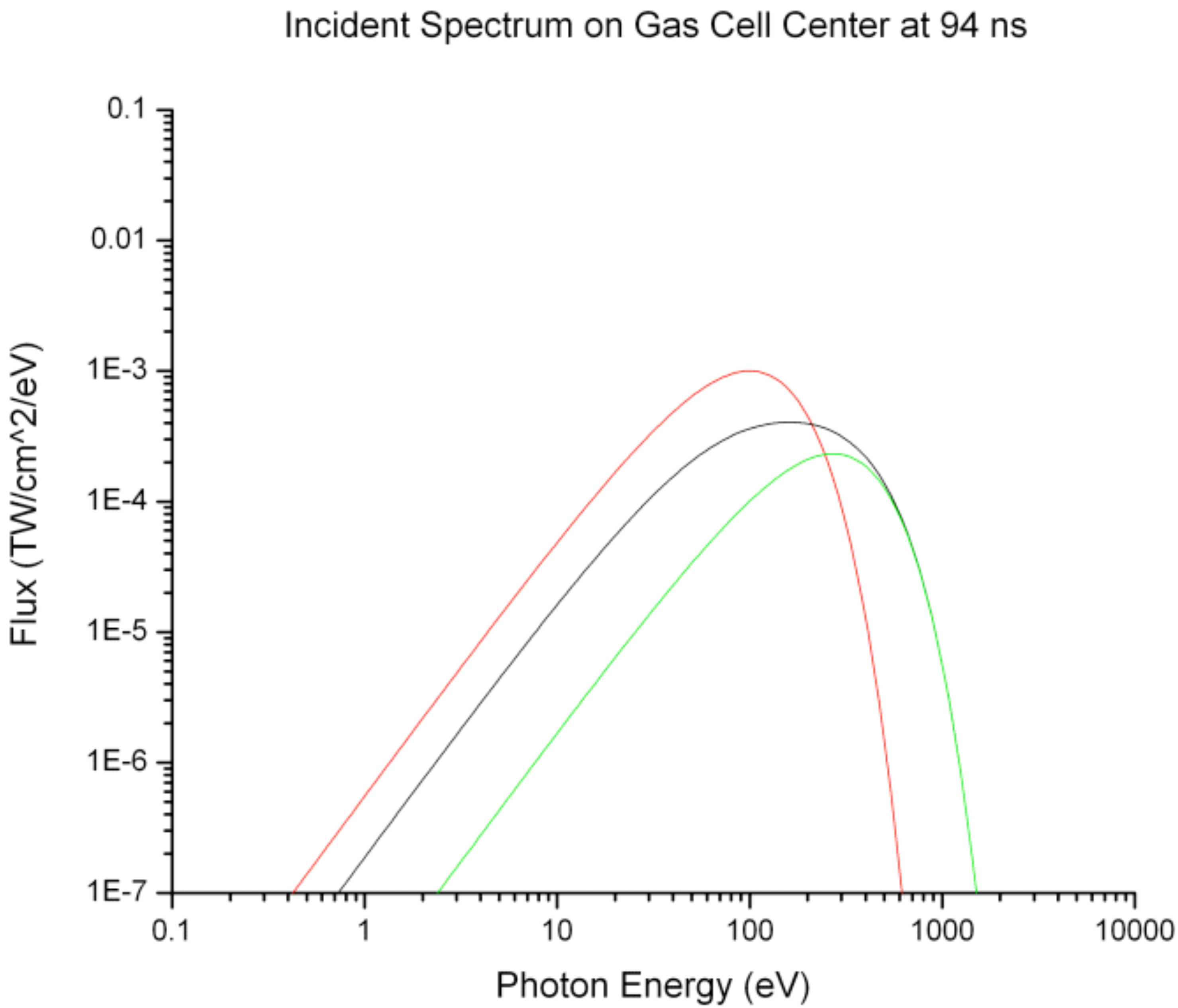

Incident Spectrum on Gas Cell Center at 94 ns
Flux (TW/cm^2/eV)
0.1
0.01
1E-3
1E-4
1E-5
1E-6
1E-7
0.1
1
10
100
1000
10000
Photon Energy (eV)

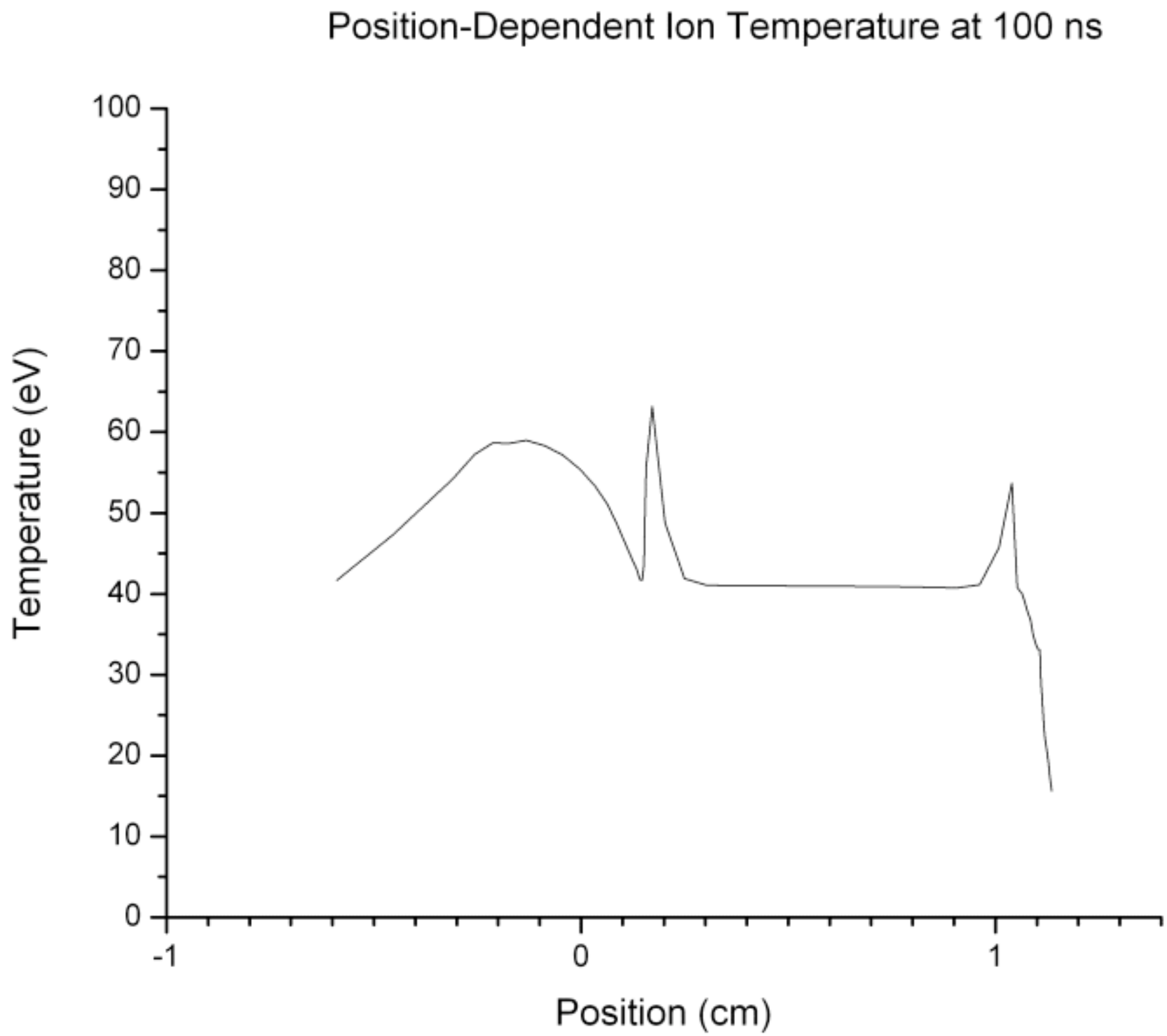

Position-Dependent Ion Temperature at 100 ns
Temperature (eV)
100
90
80
70
60
50
40
30
20
10
0
-1
0
1
Position (cm)

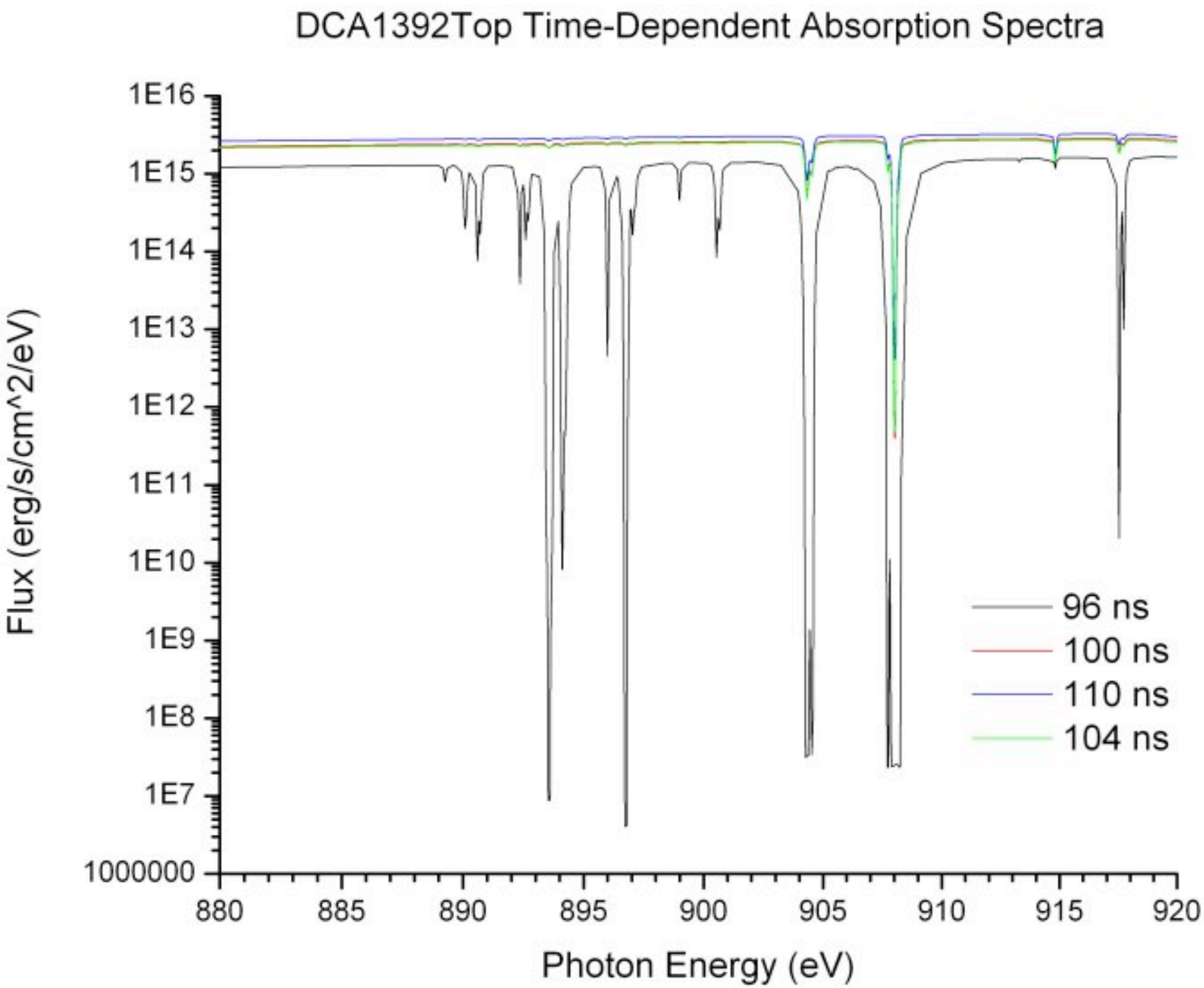

DCA1392Top Time-Dependent Absorption Spectra
Flux (erg/s/cm^2/eV)
1E16
1E15
1E14
1E13
1E12
1E11
1E10
1E9
1E8
1E7
1000000
880
885
890
895
900
905
910
915
920
Photon Energy (eV)
96 ns
100 ns
110 ns
104 ns

TREX* spectrometers record time-integrated and gated spectra

- Two sets of brass plates, aluminum wedges and steel spoolers were fabricated at the UNR Physics machine shop customized for new KAP crystals

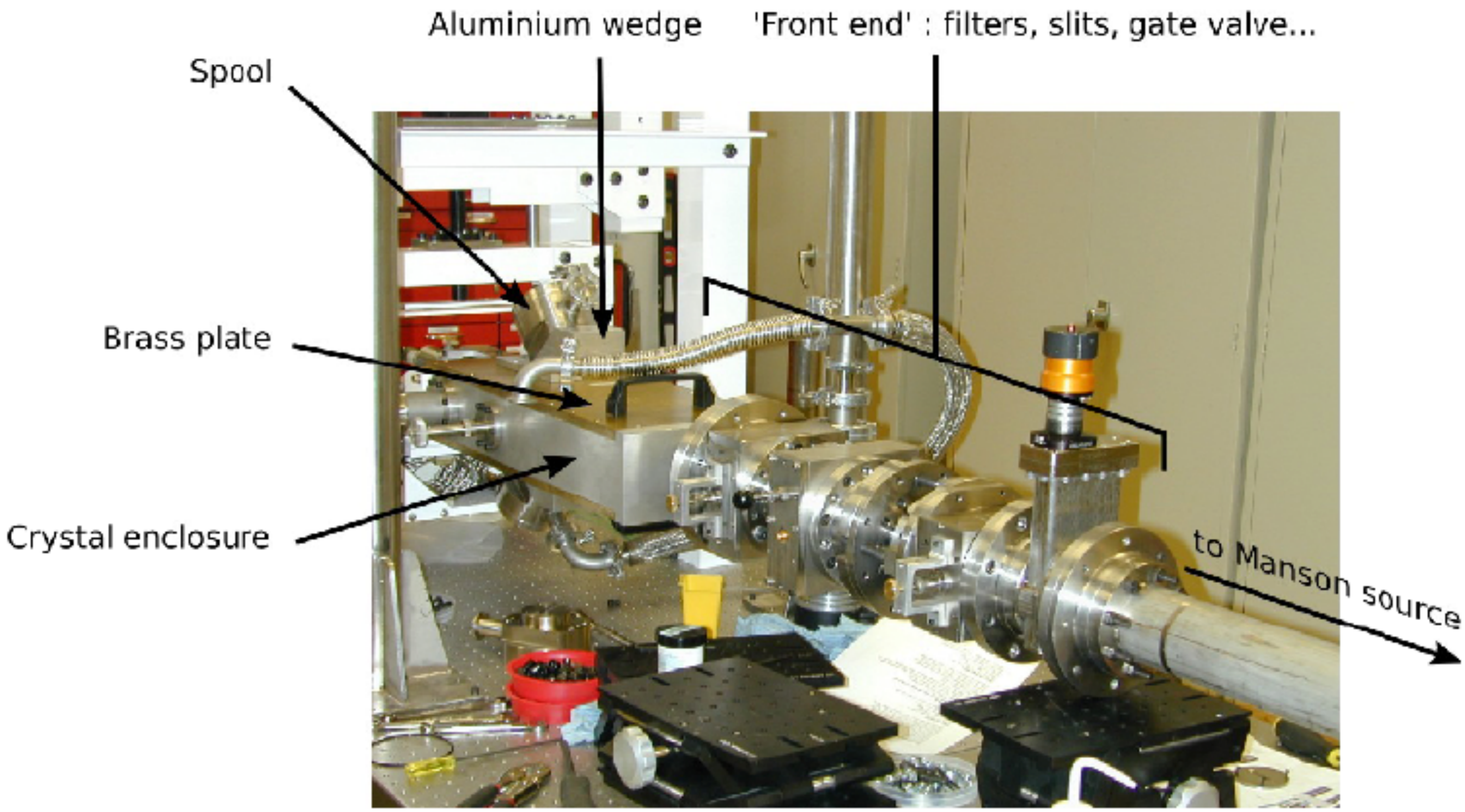

* P.W. Lake, J.E. Bailey et al, Rev. Sci. Instrum. **75**, 3690 (2004); P.W. Lake, J.E. Bailey et al, Rev. Sci. Instrum. **77**, 10F315 (2006)

Transmission spectrum through Ne photoionized plasma

- $N_e = 8 \times 10^{18}\ cm^{-3}$
- $T_e = 10$ eV
- $T_b = 45$ eV
- $T_c = 200$ eV

- Line transitions:
  - $1s^1 - 2p^1$ (Lyα)
  - $1s^1 - 3p^1$ (Lyβ)
  - $1s^2 - 1s^1\ 2p^1$ (Heα)
  - $1s^2 - 1s^1\ 3p^1$ (Heβ)
  - $1s^2 - 1s^1\ 4p^1$ (Heγ)
  - $1s^2 - 1s^1\ 5p^1$ (Heδ)
  - $1s^2 - 1s^1\ 6p^1$ (Heε)
  - $1s^2 - 1s^1\ 7p^1$
  - $1s^2 - 1s^1\ 8p^1$
  - $1s^2 - 1s^1\ 9p^1$
  - $1s^2 - 1s^1\ 10p^1$
  - $1s^2\ 2L - 1s^1\ 2L\ np^1$ (n=3-10)

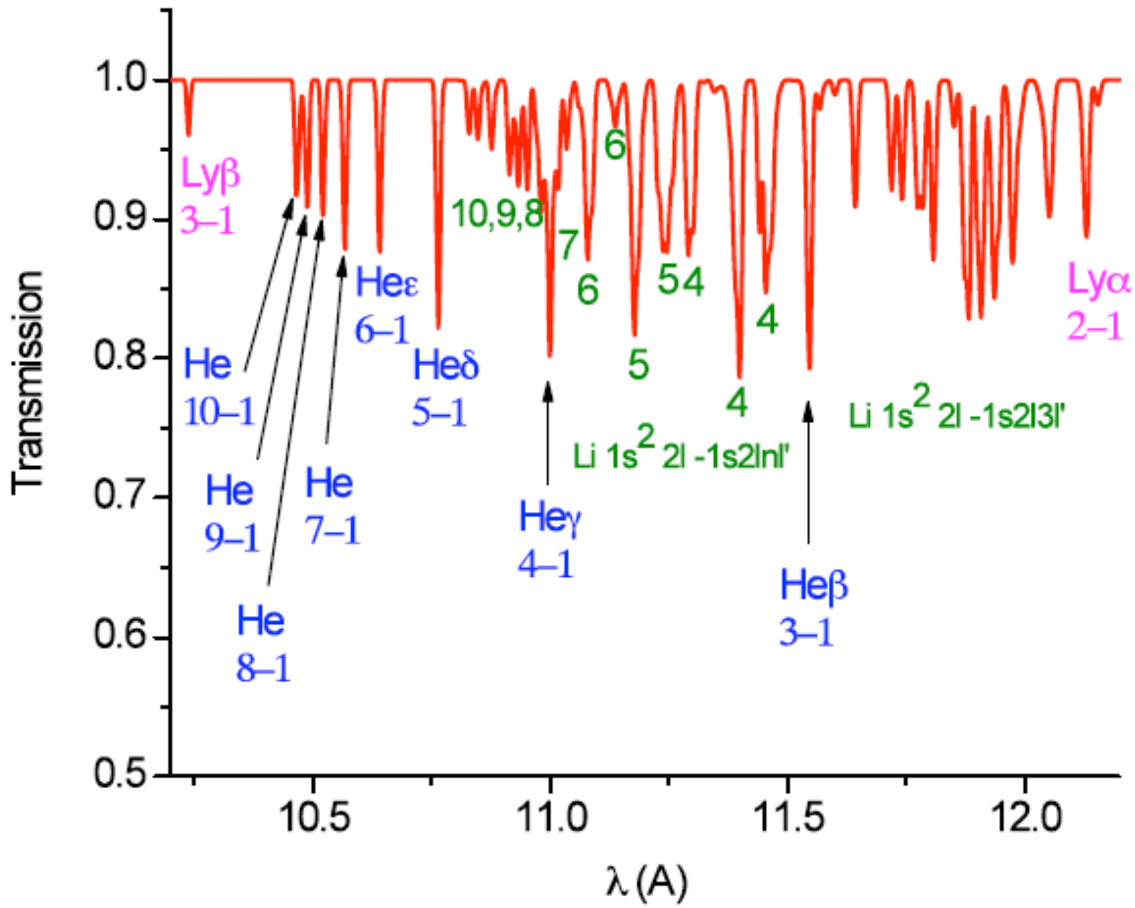

Progression of ξ in Z photoionized plasma experiments is impressive:

- Side gas cell[1]: $\xi = 5 - 7 \text{ erg} \cdot \text{cm} / \text{s}$
- Expanding foil[2]: $\xi = 20 - 25 \text{ erg} \cdot \text{cm} / \text{s}$
- Top gas cell[3]: $\xi = 100 - 600 \text{ erg} \cdot \text{cm} / \text{s}$

Large values of ξ help us achieve two goals:

- investigate new and challenging laboratory plasmas
- increase relevance of laboratory plasma for astrophysics

[1]J.E. Bailey et al, J. Quant. Spectrosc. Radiative Transfer **71**, 157 (2001), and current experiments
[2]M.E. Foord et al, Phys. Rev. Letters **93**, 055002 (2004)
[3]New design for future experiments

Stark broadening effect can dominate line width

- Full width half maximum of Voigt line profile, natural and Doppler broadening
- Full width half maximum of Stark-broadened He-like neon series line profiles
- Stark width increases with *n*

$N_a = 1\times10^{18} cm^{-3}$

$N_e = 8\times10^{18} cm^{-3}$

$T_e = T_i = 30 eV$

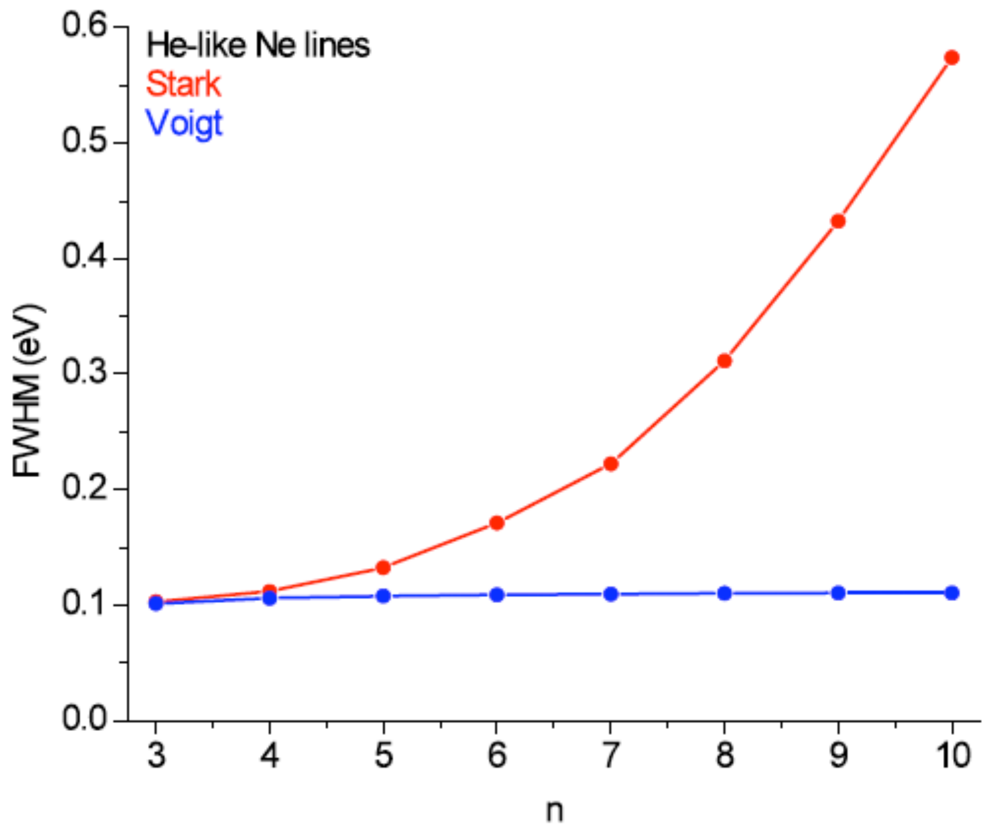

Theoretical fit to the experimental transmission

Population number densities:

$N(1s^2\,2s) = 3.6 \times 10^{16}\ cm^{-3}$

$N(1s^2\,2p) = 3.6 \times 10^{16}\ cm^{-3}$

$N(1s^2) = 1.98 \times 10^{18}\ cm^{-3}$

$N(1s) = 1.4 \times 10^{16}\ cm^{-3}$

$Na \approx 2.1 \times 10^{18}\ cm^{-3}$

H-like Ne Lyβ (1-3) is very weak

No evidence of line transitions in Be-like Ne

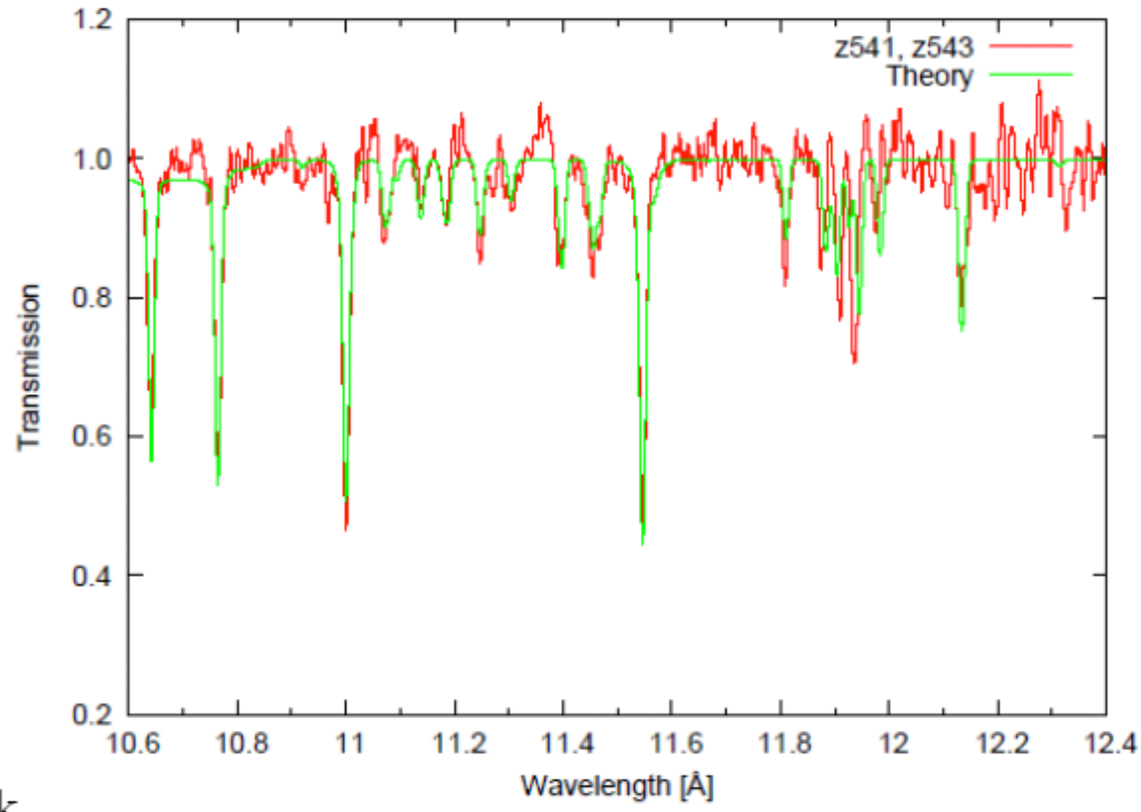

Genetic algorithm – forward modeling to extract CSD

Charge state distribution (CSD) analysis results

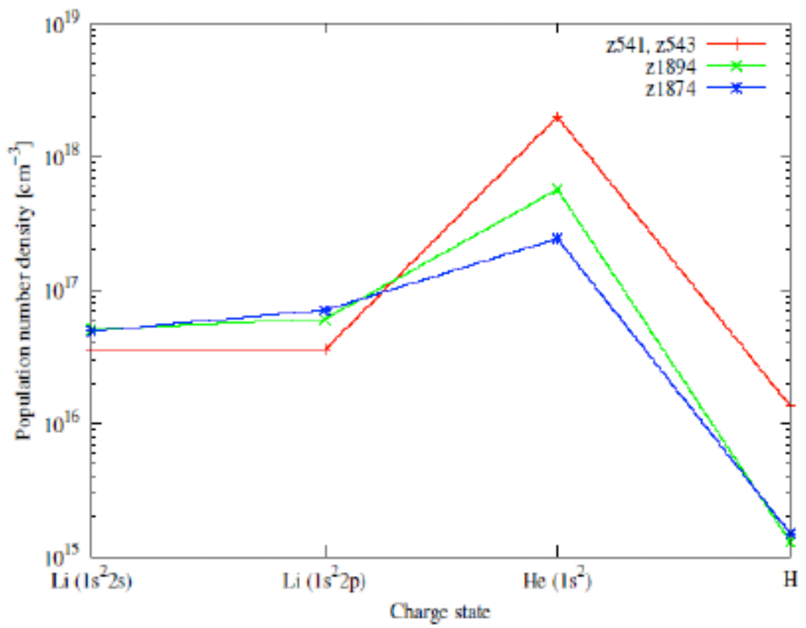

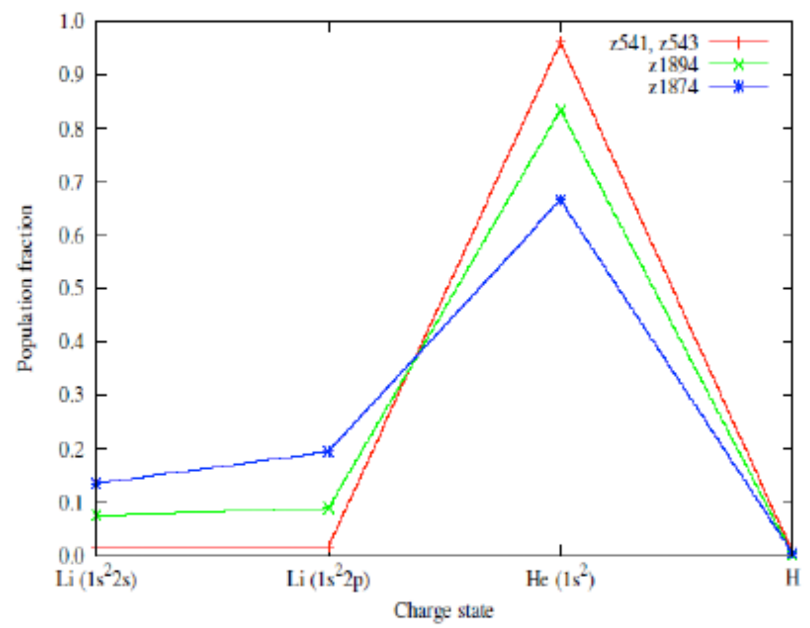

Complementary: Curve of Growth analysis (in progress)

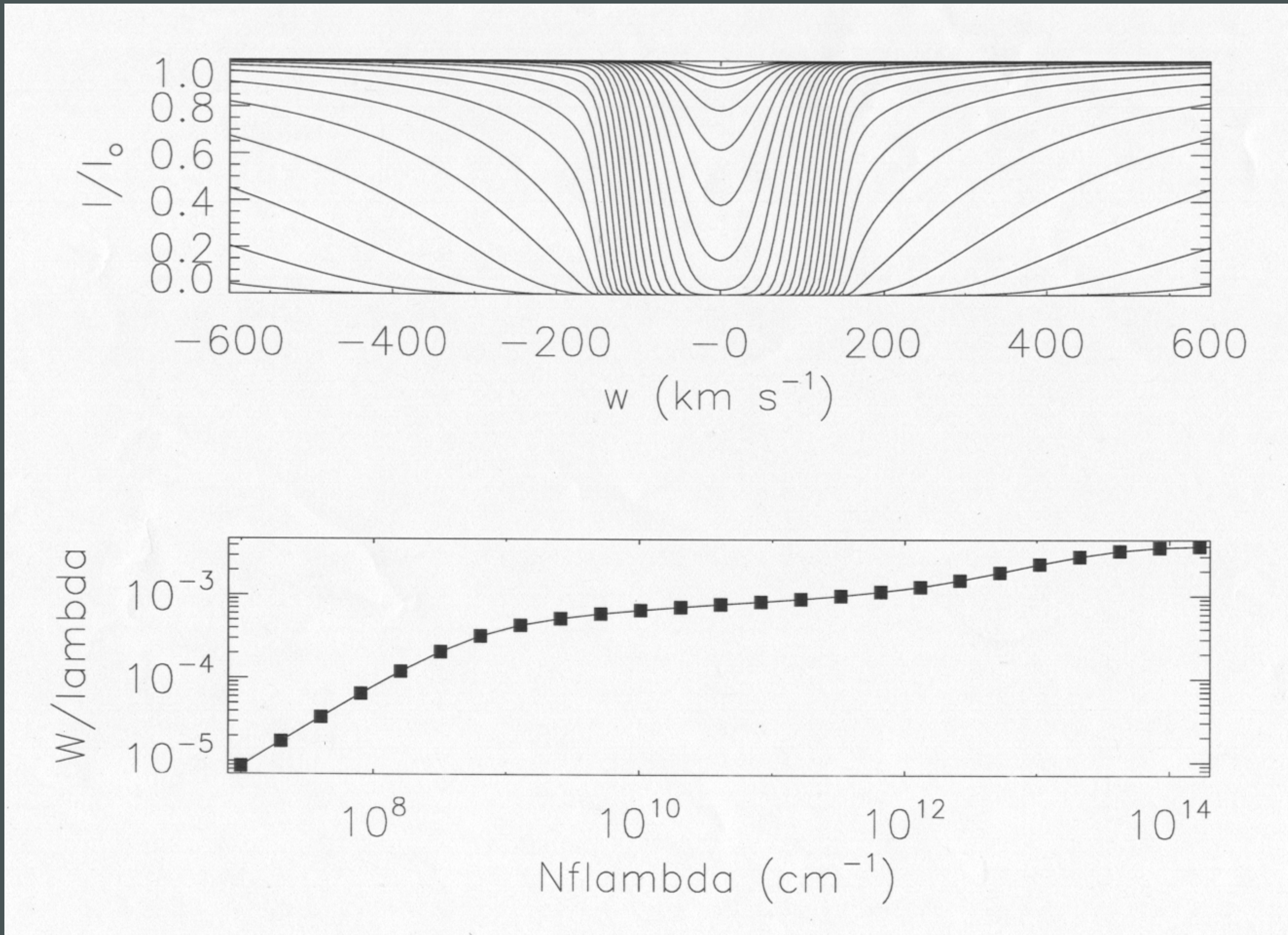

We model the CSD with *PrismSpect* and with *CLOUDY*

Adjust incident spectrum to match experimental results with simulations

We model the CSD with *PrismSpect* and with *CLOUDY*

Adjust incident spectrum to match experimental results with simulations

Both codes reproduce the CSD, but with different radiation fields – the calculated ionization parameters differ by 50%

Connections to astrophysics

Code benchmarking – what CSD, temperature arise from a given ionization parameter?

Atomic physics – wavelengths, line broadening, even *line identification*

A&A 365, L168–L173 (2001)
DOI: 10.1051/0004-6361:20000081

Astronomy & Astrophysics

Complex resonance absorption structure in the X-ray spectrum of IRAS 13349+2438*

M. Sako[1], S. M. Kahn[1], E. Behar[1], J. S. Kaastra[2], A. C. Brinkman[2], Th. Boller[3], E. M. Puchnarewicz[4], R. Starling[4], D. A. Liedahl[5], J. Clavel[6], and M. Santos-Lleo[6]

[1] Department of Physics and Columbia Astrophysics Laboratory, 550 West 120th Street, New York, NY 10027, USA
[2] Space Research Organization of the Netherlands, Sorbonnelaan 2, 3548 CA, Utrecht, The Netherlands
[3] Max-Planck-Institut fuer Extraterrestrische Physik, Postfach 1603, 85741 Garching, Germany
[4] Mullard Space Science Laboratory, University College, London, Holmbury St. Mary, Dorking, Surrey, RH5 6NT, UK
[5] Physics Department, Lawrence Livermore National Laboratory, PO Box 808, L-41, Livermore, CA 94550, USA
[6] XMM Science Operations, Astrophysics Division, ESA Space Science Dept., PO Box 50727, 28080 Madrid, Spain

Received 2 October 2000 / Accepted 30 October 2000

Abstract. The luminous infrared-loud quasar IRAS 13349+2438 was observed with the *XMM-Newton* Observatory as part of the Performance Verification program. The spectrum obtained by the Reflection Grating Spectrometer (RGS) exhibits broad ($v \sim 1400$ km s^{-1} FWHM) absorption lines from highly ionized elements including hydrogen- and helium-like carbon, nitrogen, oxygen, and neon, and several iron L-shell ions (Fe XVII–XX). Also shown in the spectrum is the first astrophysical detection of a broad absorption feature around $\lambda = 16{-}17$ Å identified as an unresolved transition array (UTA) of 2p–3d inner-shell absorption by iron M-shell ions in a much cooler medium; a feature that might be misidentified as an O VII edge when observed with moderate resolution spectrometers. No absorption edges are clearly detected in the spectrum. We demonstrate that the RGS spectrum of IRAS 13349+2438 exhibits absorption lines from at least two distinct regions, one of which is tentatively associated with the medium that produces the optical/UV reddening.

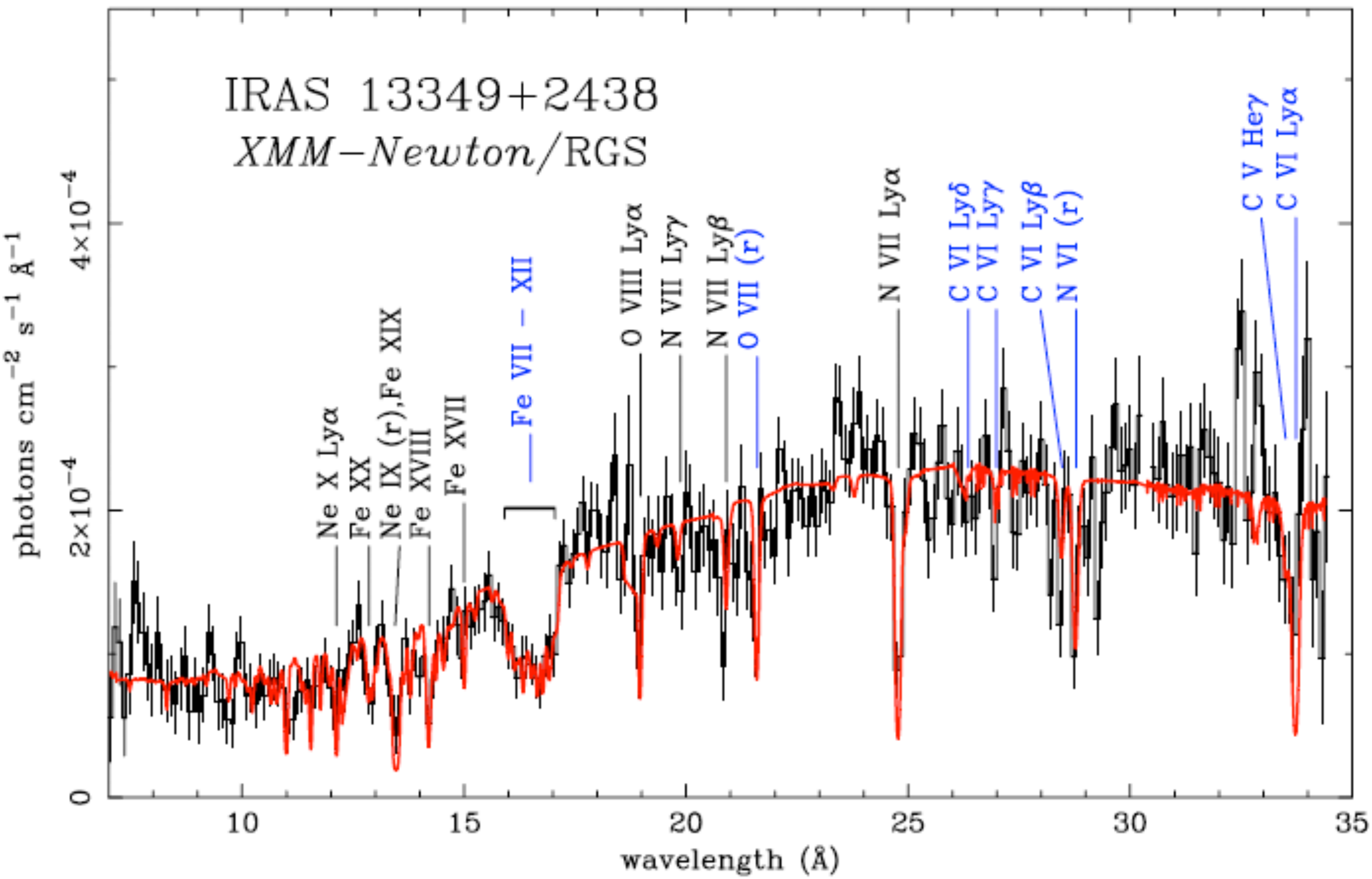
IRAS 13349+2438
XMM−Newton/RGS
photons cm⁻² s⁻¹ Å⁻¹
wavelength (Å)
Ne X Lyα
Fe XX
Ne IX (r),Fe XIX
Fe XVIII
Fe XVII
Fe VII – XII
O VIII Lyα
N VII Lyγ
N VII Lyβ
O VII (r)
N VII Lyα
C VI Lyδ
C VI Lyγ
C VI Lyβ
N VI (r)
C V Heγ
C VI Lyα

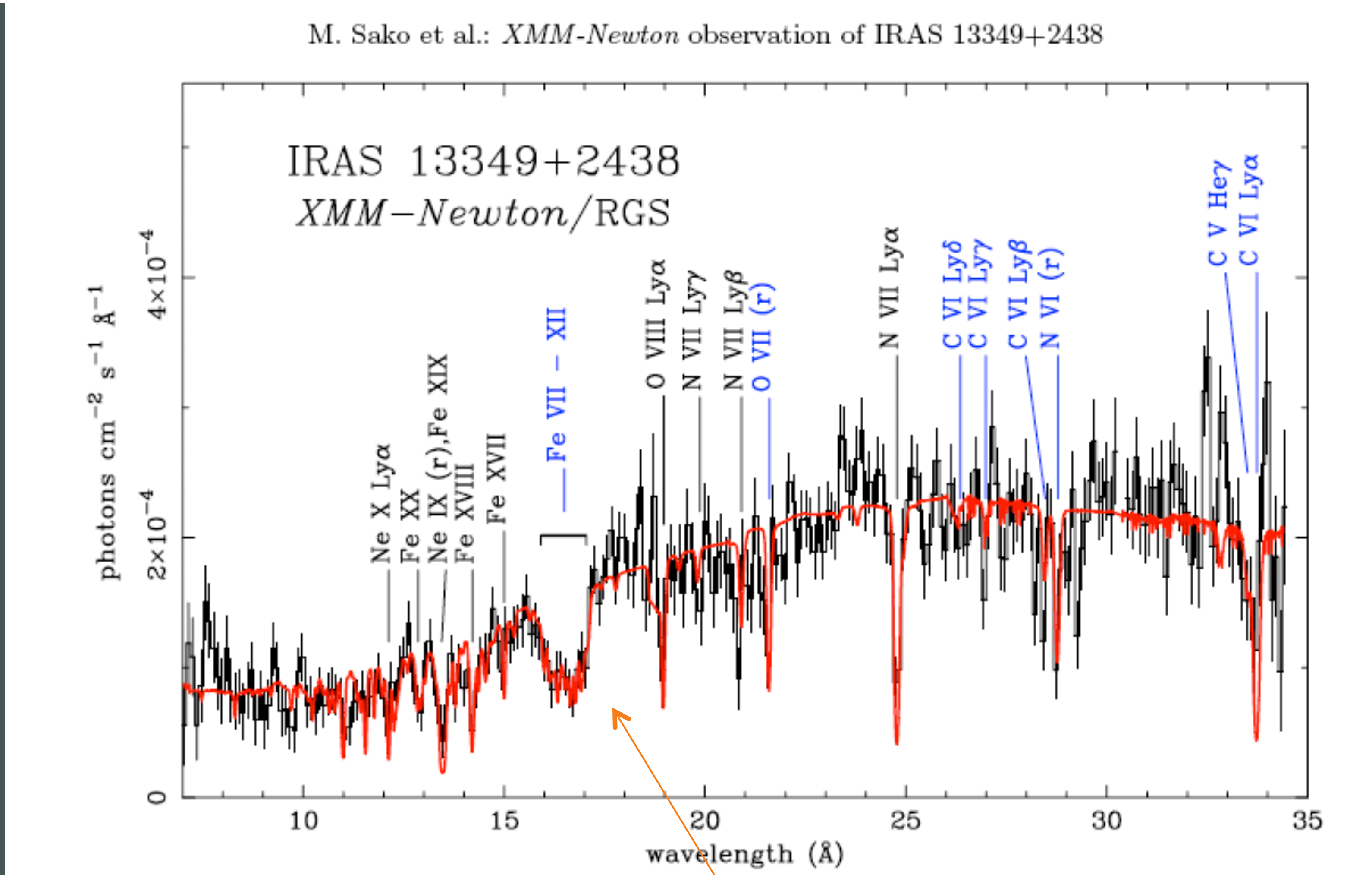

Controversy: broad Fe UTA or O K-shell edge?

Laboratory Astrophysics Needs
wavelengths & oscillator strengths

- Wind speeds are largely of a few 100 km/s =>
  - Required wavelength accuracy thus < 1/1000 (< 2 - 20 mÅ)
- Atomic codes hardly achieve such accuracy

TABLE 1

WAVELENGTHS IN Å FOR THE q, r AND β LINES IN OXYGEN

Obtained Via	Source	O VI q-r	O V β
Laboratory Measurement.......	Nicolosi & Tondello (1977)	22.020 ± 0.006	...
	LLNL EBIT[a]	22.0194 ± 0.0016	22.374 ± 0.003
Calculation	Gabriel (1972)	22.02	...
	Vainshtein & Safronova (1971, 1978)	22.02	22.38
	Chen (1985, 1986)	22.06	22.41
	Behar & Kahn (2002)	22.00	22.33
	Pradhan et al. (2003)	22.05	22.35
Observation	NGC 5548[b]	22.01 ± 0.01	22.38 ± 0.01

[a] This work.
[b] J. Kaastra 2003, private communication; adjusted for outflow velocity derived from the O VII K-shell lines.

- How reliable are the computed photo-absorption cross sections $\sigma \sim f_{ij}$?

Courtesy: E. Behar

Connections to astrophysics

Code benchmarking – what CSD, temperature arise from a given ionization parameter?

Atomic physics – wavelengths, line broadening, even *line identification*

Difficulties

If lab system is integrated (e.g. hydro important in the photoionization experiments) it's never in the way that's relevant to integrated astrophysical problem.

Regimes are difficult to match (e.g. densities too high).

Timescales and equilibrium.

Sociological/communication issues – delivering the information astrophysicists already (know they) want.

Needs and future prospects

Specifically for photoionization experiments

More X-ray power/flux and higher ionization parameters

Current/future experiments at Z combine previous and new neon gas cell designs, and better diagnostics

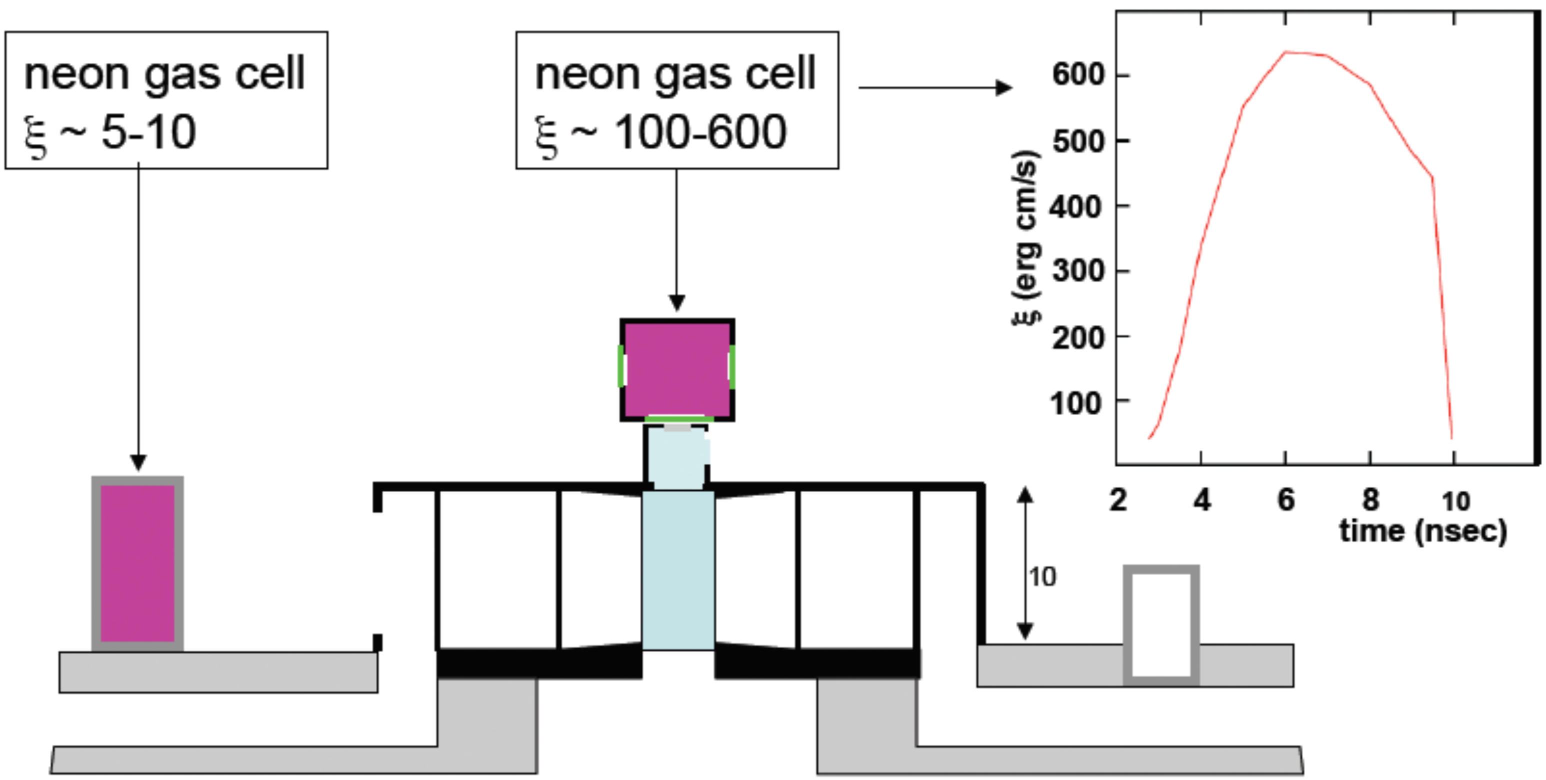

<u>Diagnostics:</u>

Emission spectroscopy – test line ratio and width signatures used by astronomers
Absorption spectroscopy – measure charge state distribution and compare models
Thomson scattering – independent temperature diagnostic
Laser interferometry – plasma density uniformity

Needs and future prospects

Specifically for photoionization experiments

More X-ray power/flux and higher ionization parameters

More and better diagnostics

Current/future experiments at Z combine previous and new neon gas cell designs, and better diagnostics

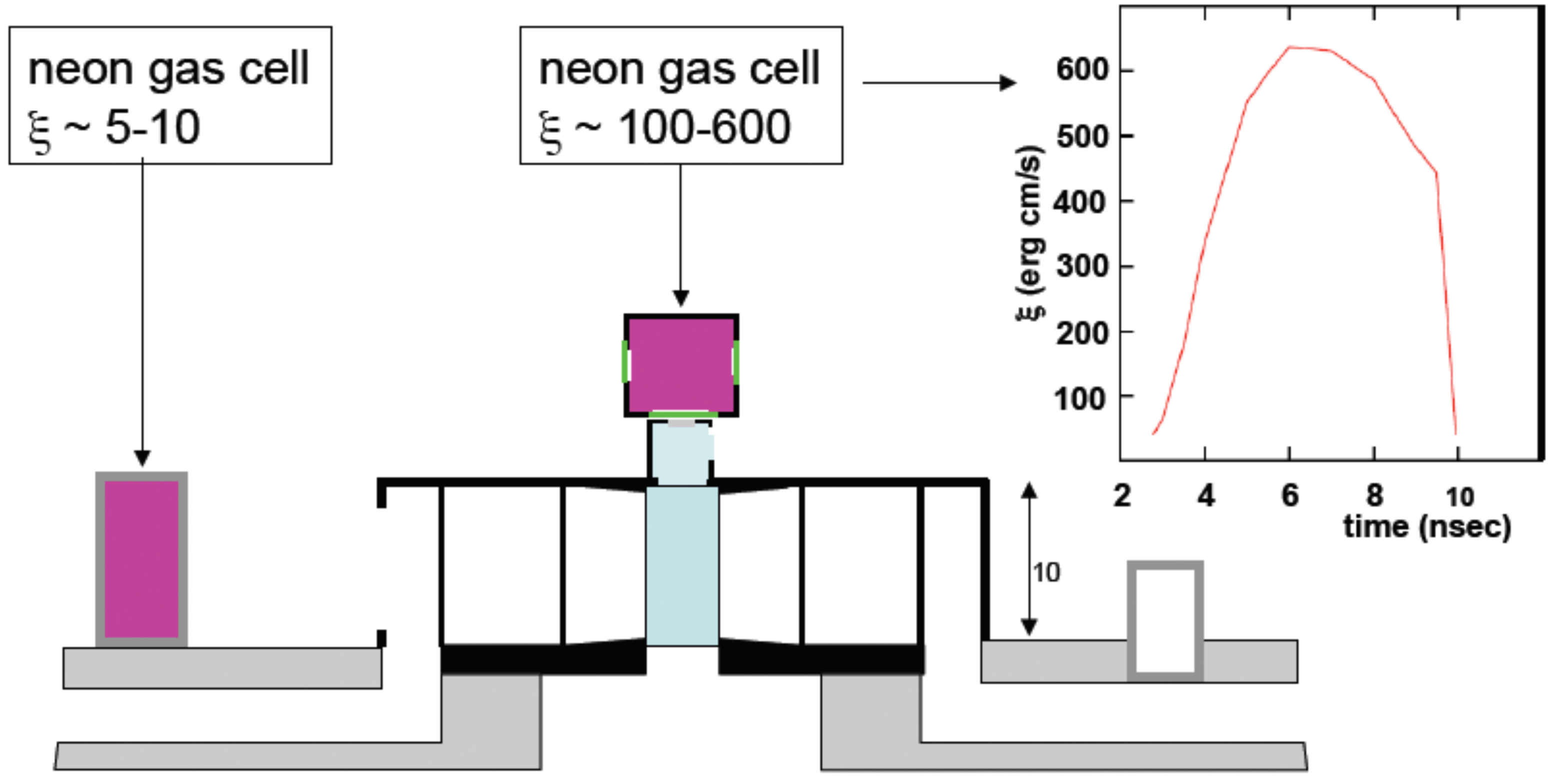

Diagnostics:

Emission spectroscopy – test line ratio and width signatures used by astronomers
Absorption spectroscopy – measure charge state distribution and compare models
Thomson scattering – independent temperature diagnostic
Laser interferometry – plasma density uniformity

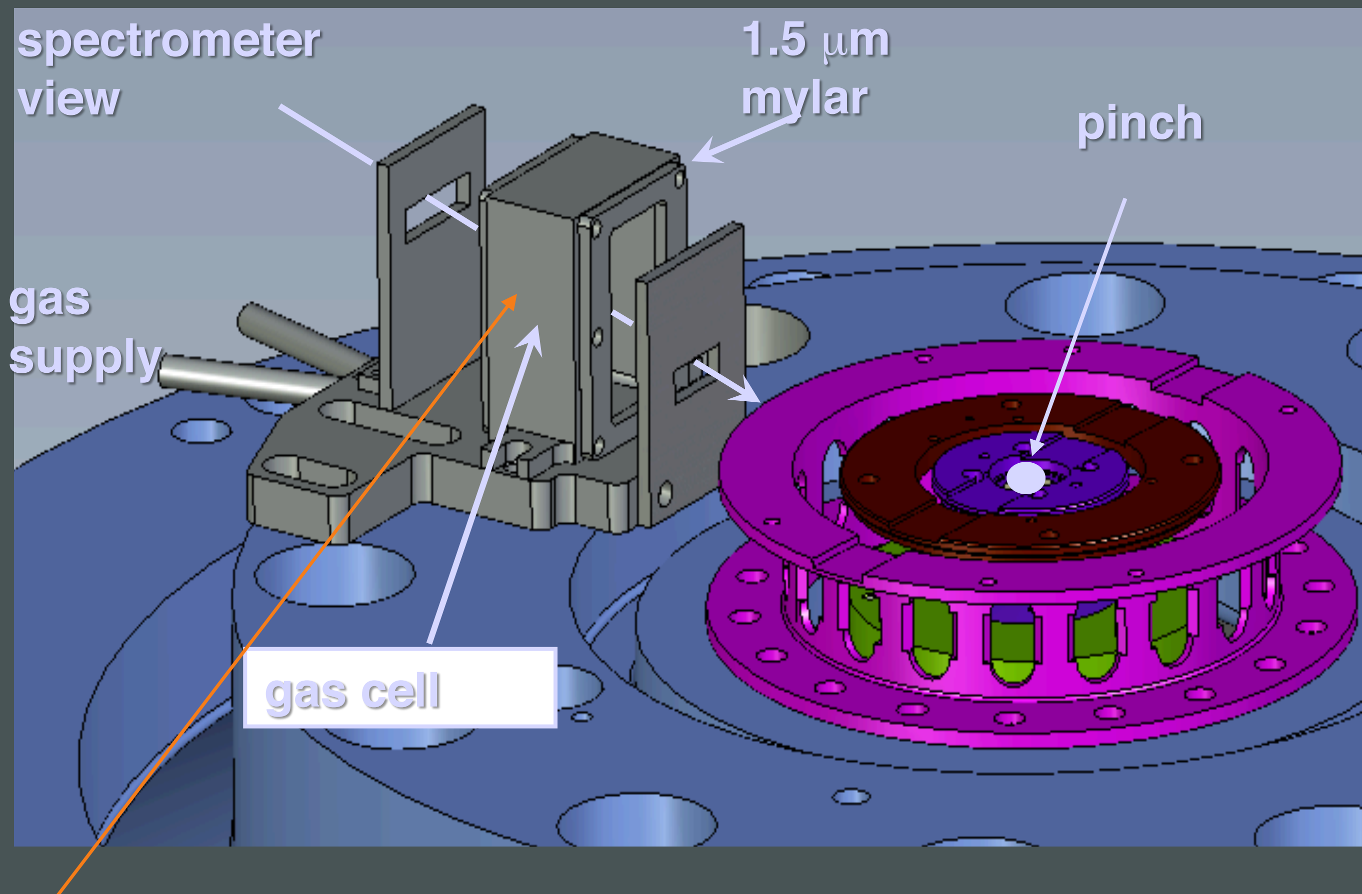

Side view with second spectrometer – measure recombination spectrum

Needs and future prospects

Specifically for photoionization experiments

More X-ray power/flux and higher ionization parameters

More and better diagnostics

Different materials (e.g. iron, but gaseous ?)

Are there relevant experiments that can be done at NIF?

Launched 2000: superior
sensitivity,
spatial resolution, and
spectral resolution

Chandra

sub-arcsecond resolution

XMM-Newton

XMM-Newton

Chandra

Both have CCD detectors for imaging spectroscopy:

low spectral resolution: $R \sim 20$ to 50

And both have grating spectrometers: $R \sim$ few 100 to 1000

300 km/s

XMM-Newton

Chandra

The gratings have poor sensitivity…
We'll never get spectra for more than a handful of any particular class of object

XMM-Newton

Chandra

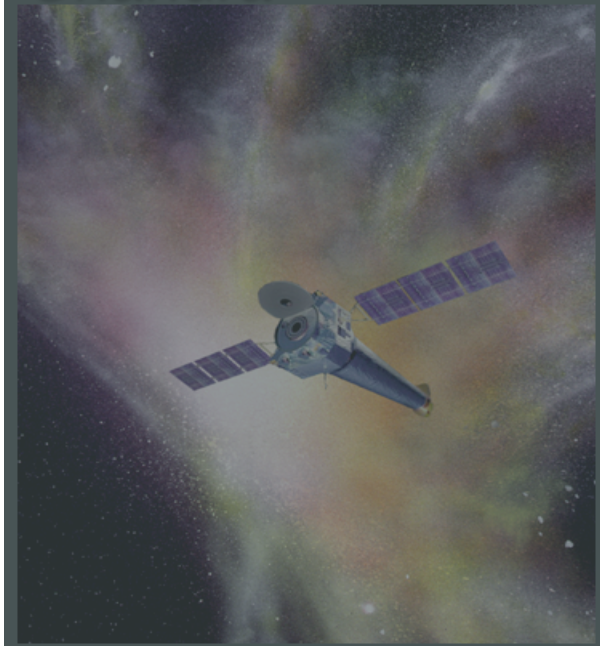

The Future:

Astro-H (Japan) – high spectral resolution at high photon energies …few years from now:
2 eV at 7 keV (microcalorimeter array)

International X-ray Observatory (IXO; US&Europe)… ~ 2020

Focus on iron K-shell

Conclusions

X-ray photoionization experiments are producing results

…higher X-ray fluxes (and ionization parameters) are required for direct astrophysical relevance.

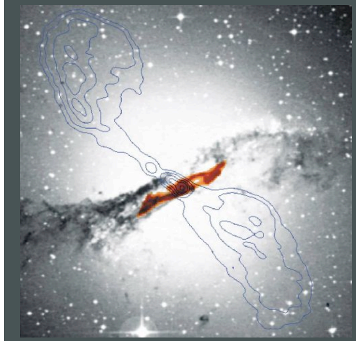

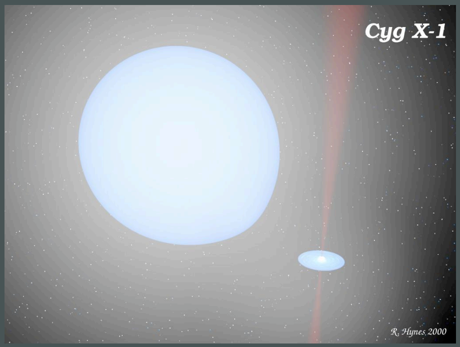

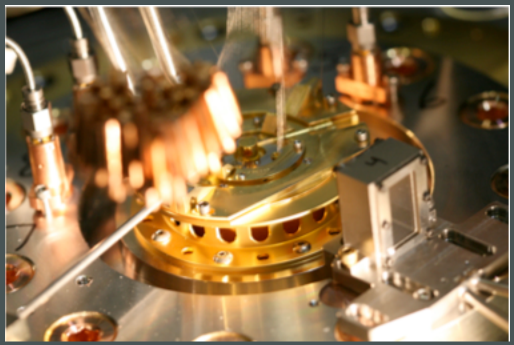

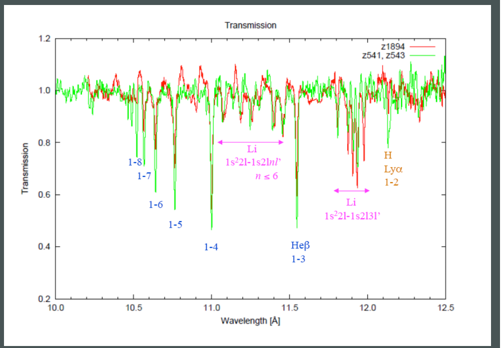

Comments on some other lab astro experiments

PHYSICAL REVIEW E VOLUME 62, NUMBER 6 DECEMBER 2000

Experiments on radiative collapse in laser-produced plasmas relevant to astrophysical jets

K. Shigemori,[1,2] R. Kodama,[1] D. R. Farley,[2] T. Koase,[1] K. G. Estabrook,[2] B. A. Remington,[2] D. D. Ryutov,[2] Y. Ochi,[1] H. Azechi,[1] J. Stone,[3] and N. Turner[3]

[1]*Institute of Laser Engineering, Osaka University, Suita, Osaka, 565-0871, Japan*

[2]*Lawrence Livermore National Laboratory, P.O. Box 808, Livermore, California 94551*

[3]*Department of Astronomy, University of Maryland, College Park, Maryland 20742*

(Received 16 May 2000)

We report a laser experiment of astrophysical interest on radiative jet formation. Conically shaped targets are irradiated by intense laser light. An ablated plasma flow collides at the axis of the cone targets, then propagates at high Mach number, forming a jetlike structure. We measure time-resolved x-ray self-emission images from the jets. The diameter of the jet increases with decreasing atomic number of the irradiated target, suggesting that the collimation is due to radiative cooling. Two-dimensional simulations reproduce essential features of the experimental results.

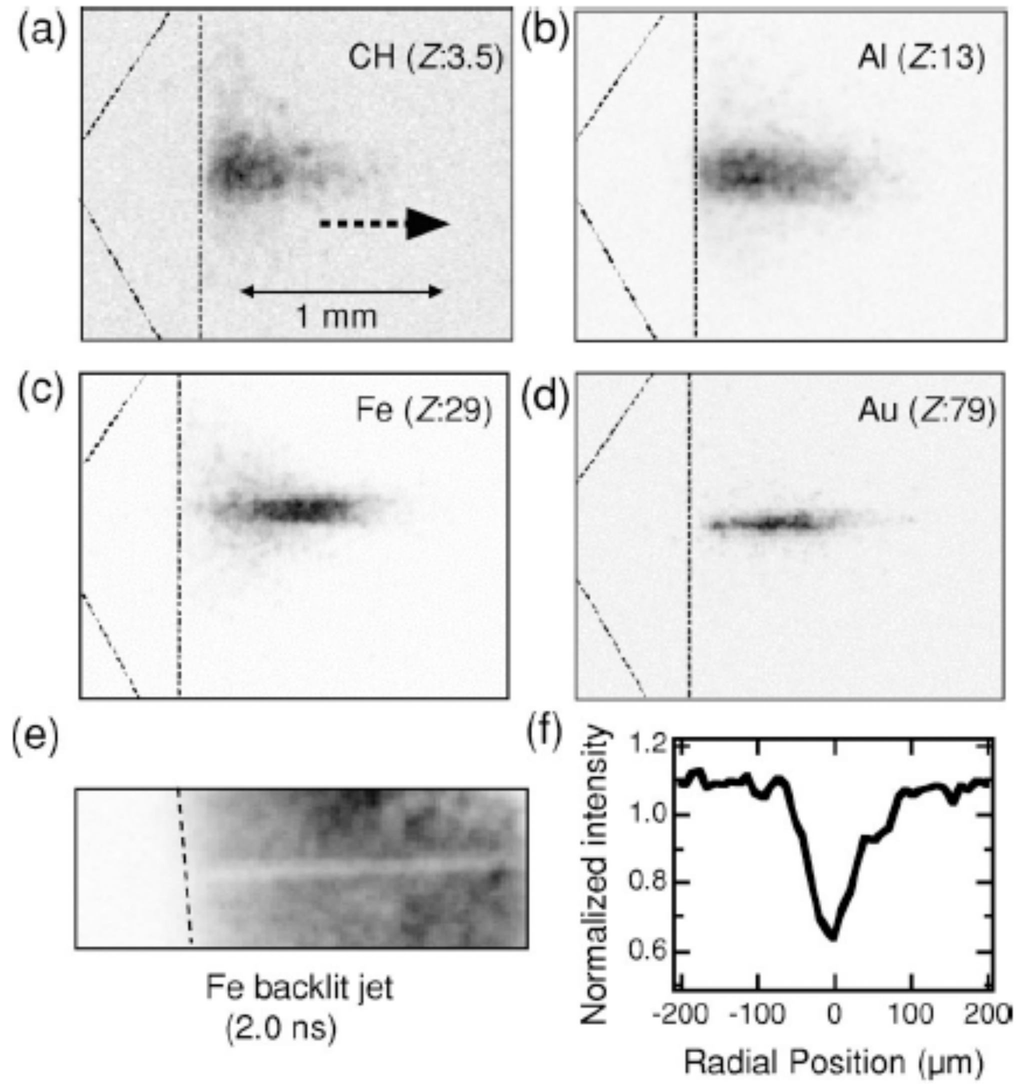

FIG. 2. Snapshots of two-dimensional side-on self-emission images from the XFC for (a) CH, (b) Al, (c) Fe, and (d) Au targets at 1.3 ns after the laser irradiation. (e) Backlit Fe jet image from the XFC at 2.0 ns, and (f) radial lineout plot at 1 mm from the center of the cone target.

38 citations to the Shigemori et al. jets paper…none are traditional astronomy

Sign on

SAO/NASA Astrophysics Data System (ADS)

Citations for 2000PhRvE..62.8838S from the ADS Databases

Go to bottom of page

The Citation database in the ADS is **NOT** complete. Please keep this in mind when using the ADS Citation lists.

Selected and retrieved **38** abstracts. (Citation History)

Sort options

#	Bibcode / Authors	Cites / Title	Date	List of Links / Access Control Help
1	2009EL.....8754005W Wang, L. F.; Ye, W. H.; Li, Y. J.	1.000 Numerical investigation on the ablative Kelvin-Helmholtz instability	09/2009	A E L R
2	2009Ap&SS.322...37G Gregory, C. D.; Howe, J.; Loupias, B.; Myers, S.; Notley, M. M.; Sakawa, Y.; Oya, A.; Kodama, R.; Koenig, M.; Falize, E.; and 3 coauthors	1.000 Colliding plasma experiments to study astrophysical-jet relevant physics	08/2009	A E L R U
3	2009Ap&SS.322...31W Waugh, J. N.; Gregory, C. D.; Wilson, L. A.; Loupias, B.; Brambrink, E.; Koenig, M.; Sakawa, Y.; Kuramitsu, Y.; Takabe, H.; Kodama, R.;	1.000 A jet production experiment using the high-repetition rate Astra laser	08/2009	A E L R U

The OP model used in solar research predicts Fe L-shell opacity that is too low at Z conditions

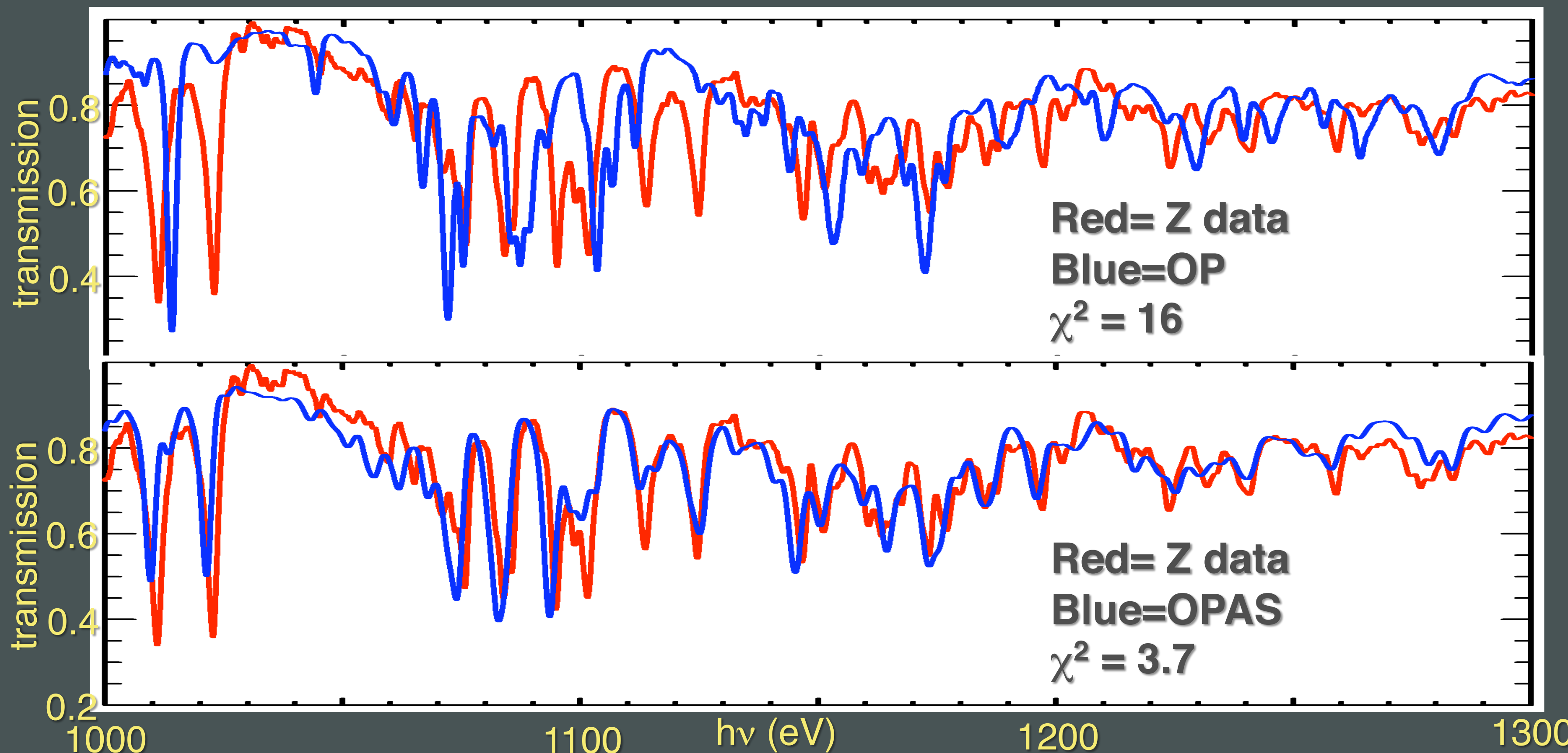

OP Rosseland mean is ~ 1.5x lower than OPAS at Z conditions.
If this difference persisted at solar conditions, it would solve the CZ problem

Courtesy: J. Bailey

Some related thoughts

THE ASTROPHYSICAL JOURNAL, 478:94–106, 1997 March 20

PROPERTIES AND SPECTROSCOPIC IMPLICATIONS OF THERMAL INSTABILITY IN X-RAY BINARY AND AGN ACCRETION FLOWS

CYNTHIA J. HESS
Department of Physics, Illinois Wesleyan University, P.O. Box 2900, Bloomington, IL 61702-2900; chess@titan.iwu.edu

AND

STEVEN M. KAHN AND F. B. S. PAERELS
Department of Physics, Pupin Hall, Columbia University, 538 West 120th Street, New York, NY 10027; skahn@carmen.phys.columbia.edu, frits@naima.phys.columbia.edu
Received 1996 July 2; accepted 1996 October 4

Helium heating-cooling balance is very important…

…so isolating one element at a time is also problematic.

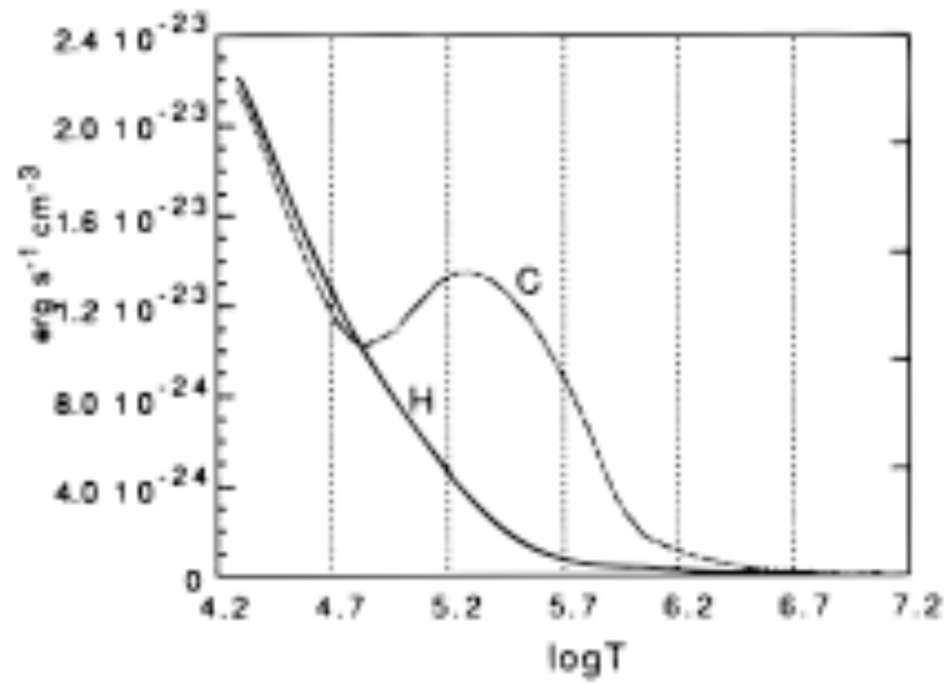

FIG. 6a

Interesting and relevant systems aren't always in the HED regime

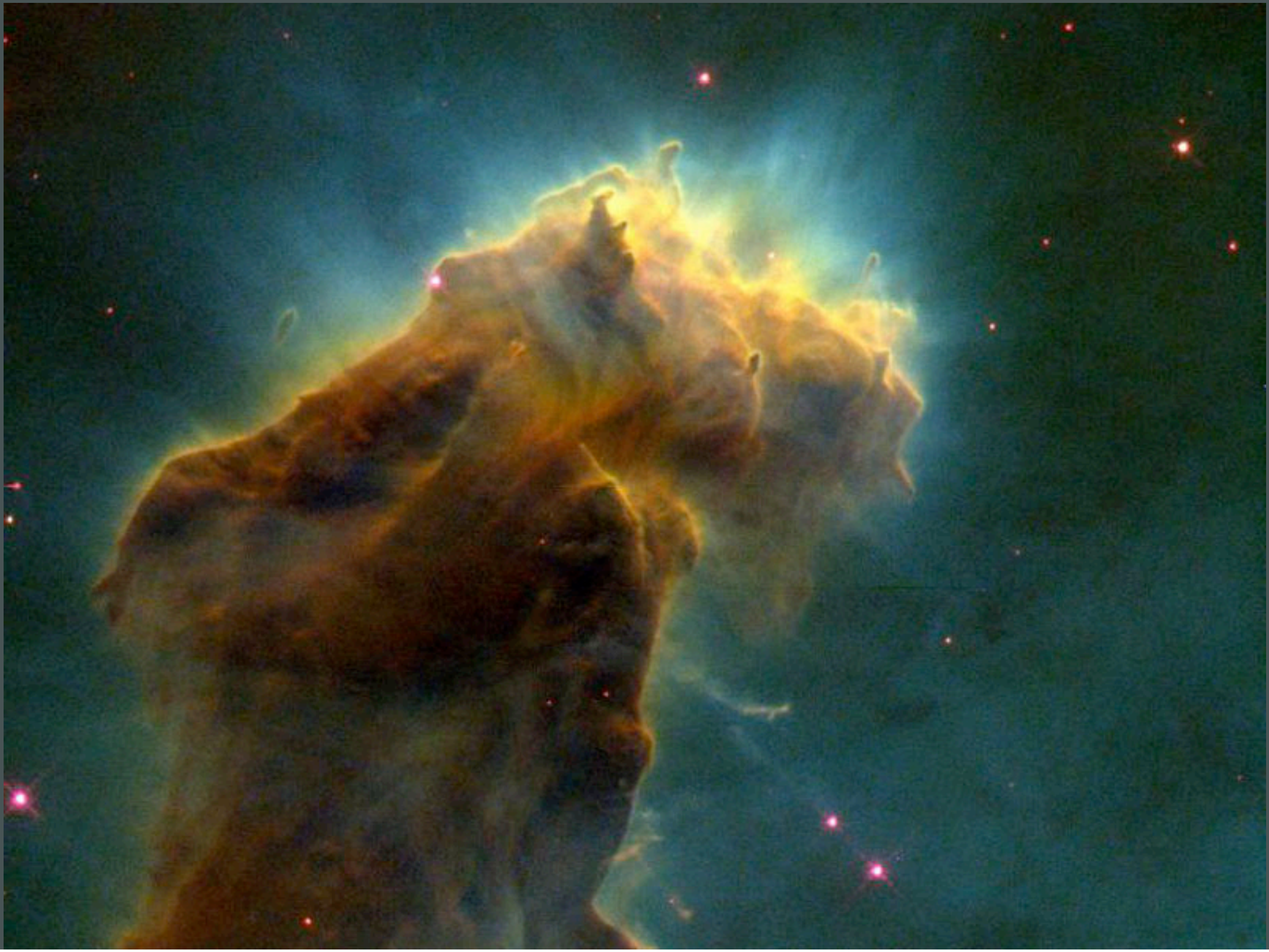

$$a_{rad} = \frac{\kappa L}{4\pi R^2 c}$$

opacity (cm²/g)

Luminosity (ergs/s)

radius

UV spectrum: C IV 1548, 1551 Å

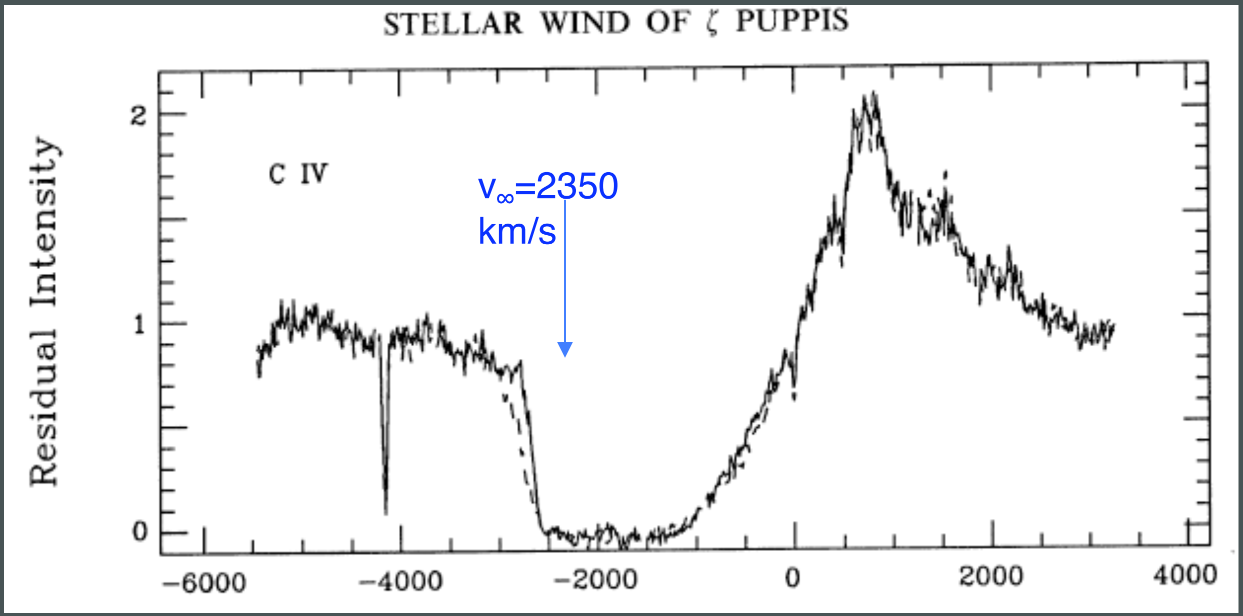

Prinja et al. 1992, ApJ, 390, 266

Velocity (km/s)

1-D rad-hydro simulation of a massive star wind

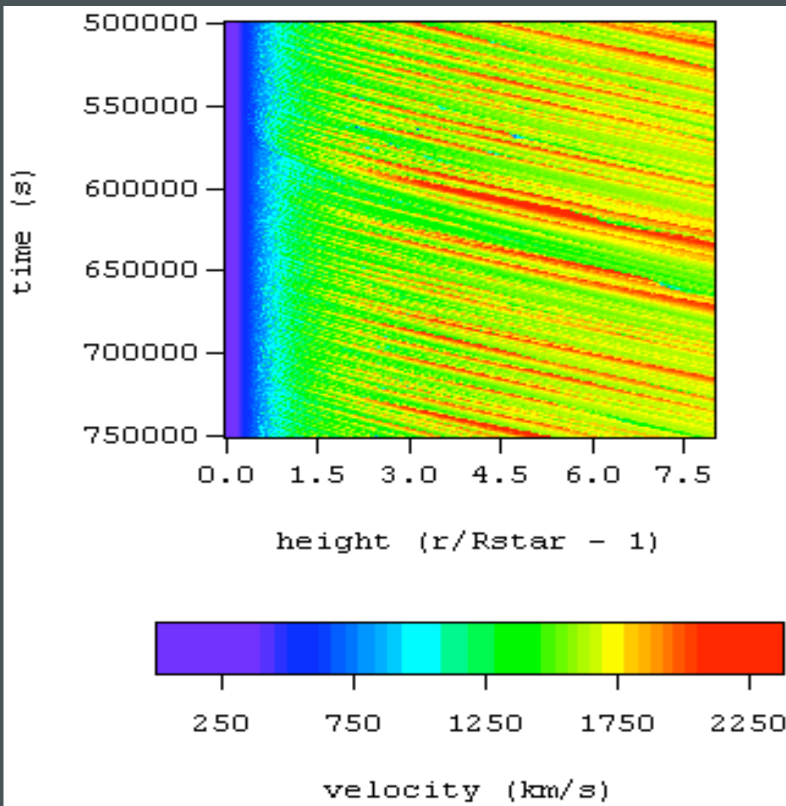

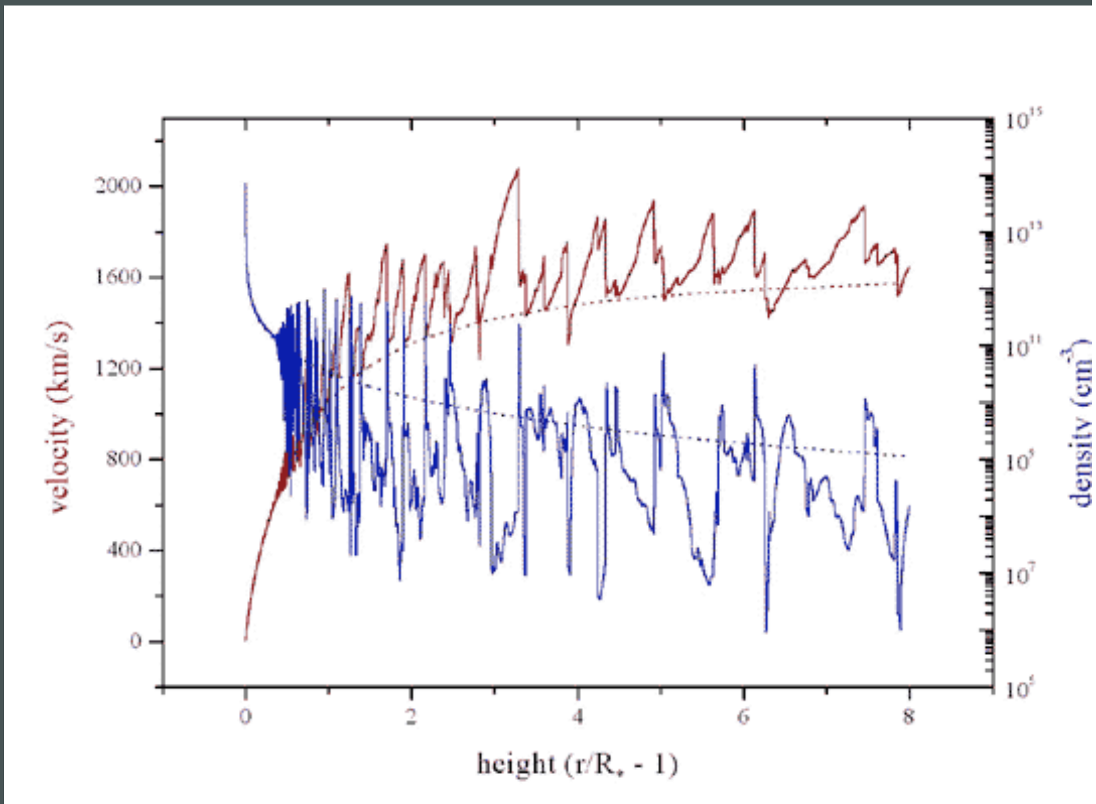

Radiation **line driving** is inherently unstable:
shock-heating and X-ray emission

Chandra HETGS/MEG spectrum
($R \sim 1000 \sim 300$ km s^{-1})

ζ Pup

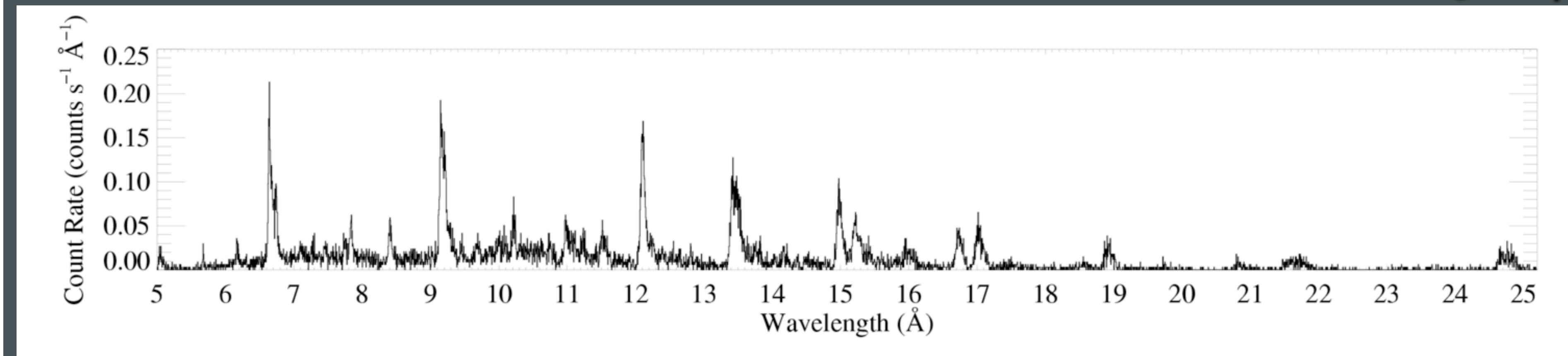

Si Mg Ne Fe O

H-like
He-like

1-D rad-hydro simulation of a massive star wind

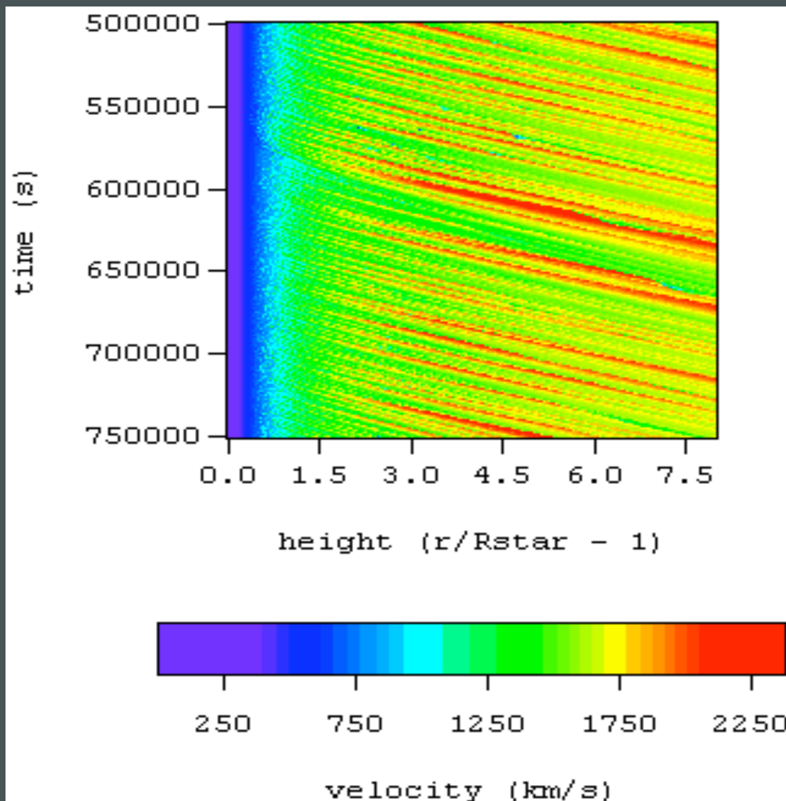

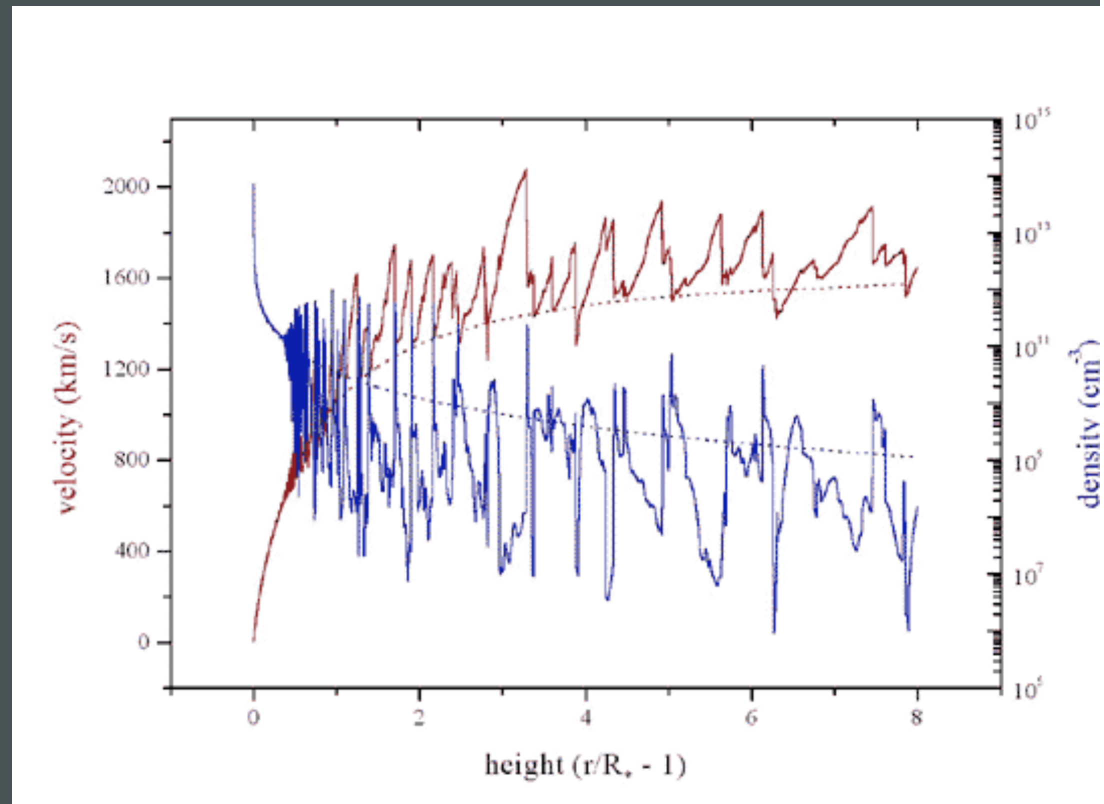

We can study clumping in these winds by watching them be blasted by x-rays from a compact object

Swarthmore Spheromak Experiment (SSX)

kT ~ 50 eV; $n_e \sim 10^{14}$; B ~ 0.1 T

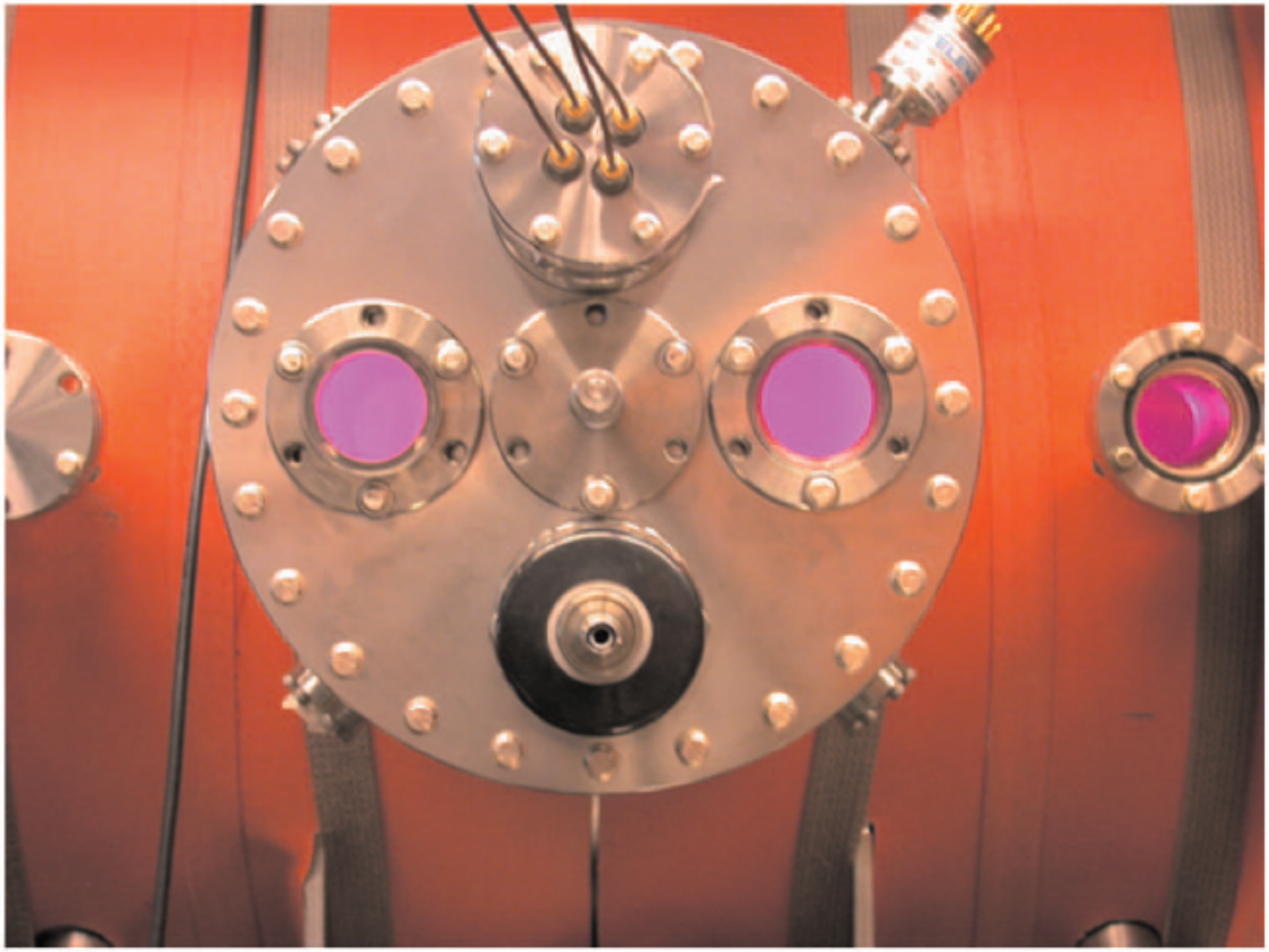

FIG. 9. (Color) Location of SXR at the midplane on the SSX machine (see the schematic in Fig. 1). The four wires at the top of the image carry current from the SXR photodiodes. Clockwise from upper left, the diodes are filtered by foils made of Al, Zr, Sn, and Ti. The port for the IDS is visible at the bottom center of this image. Note that hydrogen Balmer series recombination emission is visible through the windows in the vessel in this photograph.

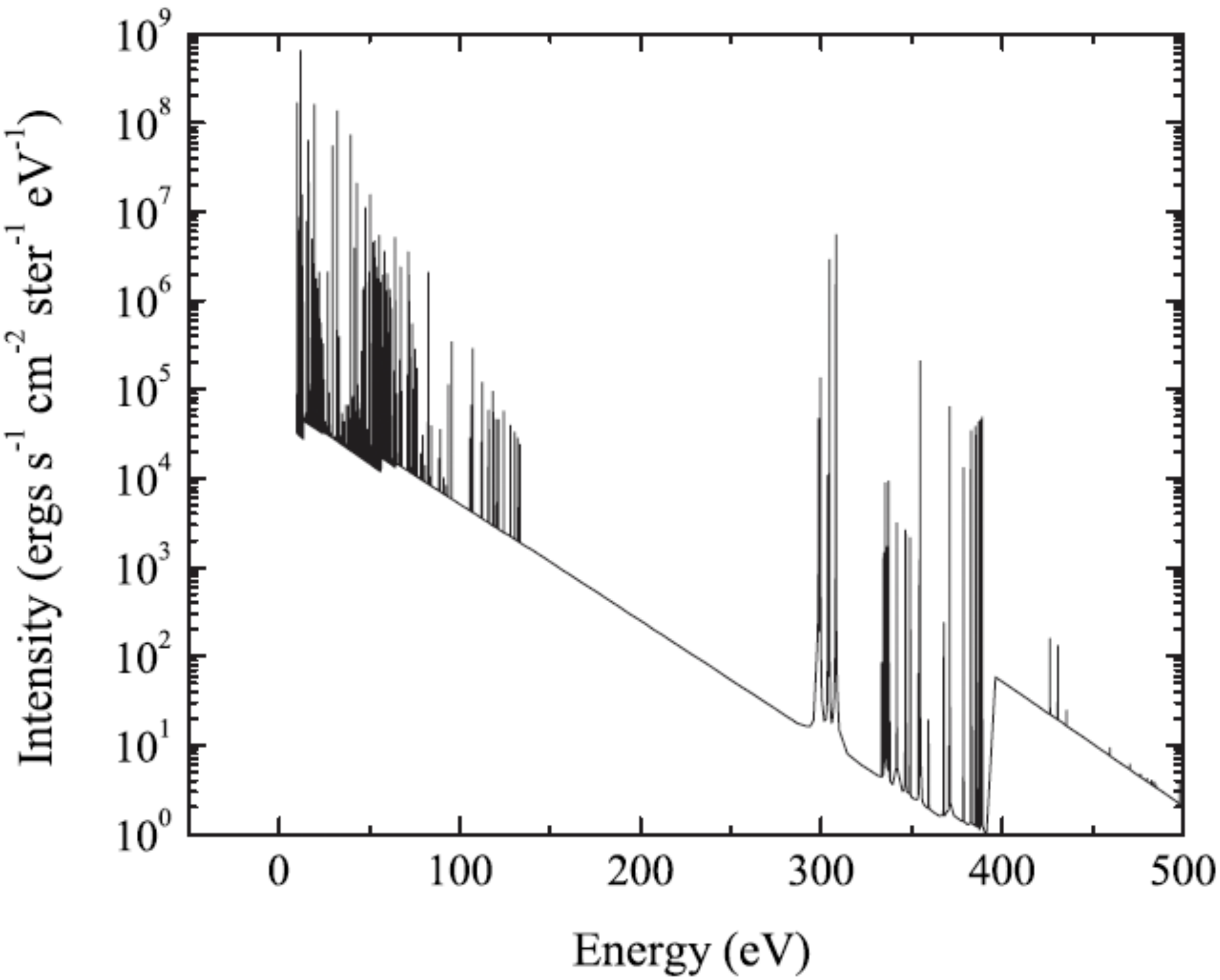

FIG. 13. Model spectrum from a steady-state simulation with $T_e = 30$ eV and $n_i = 5 \times 10^{14}$ cm^{-3}. Impurity concentrations of 1% carbon, 0.002% oxygen, and 0.003% nitrogen were included. The plasma emits primarily at $E < 150$ eV, but SXR will also measure substantial emission from the C V and C VI resonance lines between 300 and 400 eV. Note that the Zr channel has the lowest responsivity at these energies, which is counter to what is seen below 100 eV.

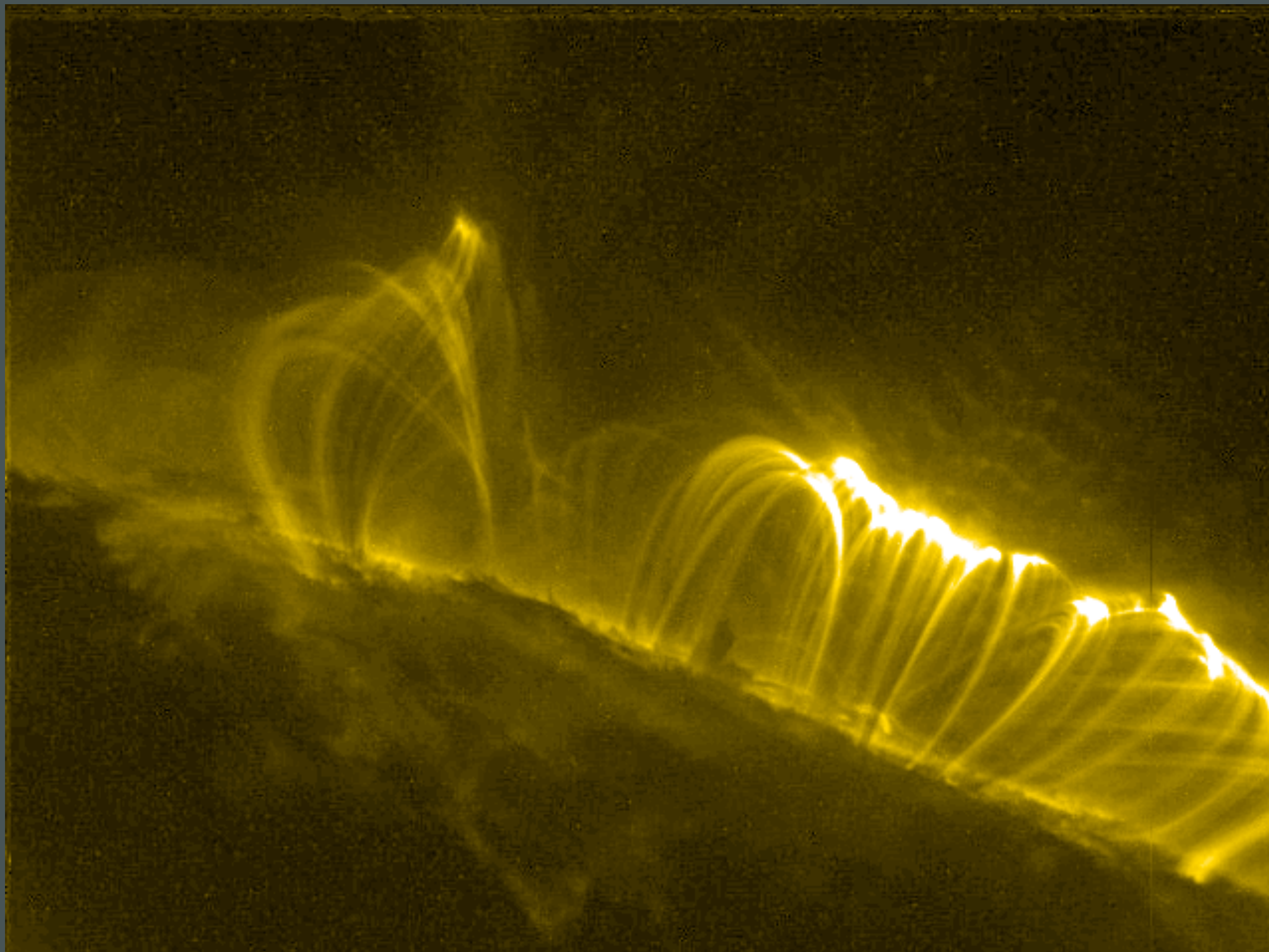

3D reconnection (lab and solar)

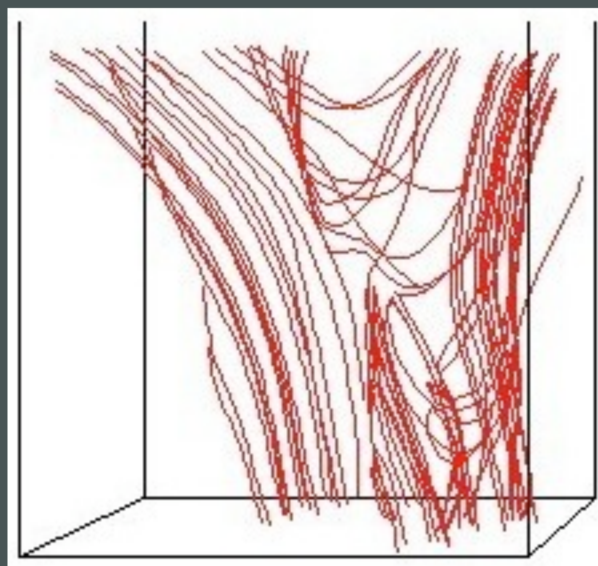

one foot tall

5 earth diameters tall

Student training and exposure to HED concepts, techniques

PHYSICS OF PLASMAS 16, 042505 (2009)

Spectroscopic measurements of temperature and plasma impurity concentration during magnetic reconnection at the Swarthmore Spheromak Experiment

V. H. Chaplin,[1,2] M. R. Brown,[1] D. H. Cohen,[1] T. Gray,[1] and C. D. Cothran[1,a)]
[1]*Department of Physics and Astronomy, Swarthmore College, Swarthmore, Pennsylvania 19081, USA*
[2]*California Institute of Technology, Pasadena, California 91125, USA*

(Received 4 November 2008; accepted 25 February 2009; published online 7 April 2009)

Electron temperature measurements during counterhelicity spheromak merging studies at the Swarthmore Spheromak Experiment (SSX) [M. R. Brown, Phys. Plasmas **6**, 1717 (1999)] are presented. VUV monochromator measurements of impurity emission lines are compared with model spectra produced by the non-LTE excitation kinematics code PRISMSPECT [J. J. MacFarlane *et al.*, in Proceedings of the Third Conference on Inertial Fusion Science and Applications (2004)] to yield the electron temperature in the plasma with 1 μs time resolution. Average T_e is seen to increase from 12 to 19 eV during spheromak merging. Average C III ion temperature, measured with a new ion Doppler spectrometer (IDS) [C. D. Cothran *et al.*, Rev. Sci. Instrum. **77**, 063504 (2006)], likewise rises during spheromak merging, peaking at ~22 eV, but a similar increase in T_i is seen during single spheromak discharges with no merging. The VUV emission line measurements are also used to constrain the concentrations of various impurities in the SSX plasma, which are dominated by carbon, but include some oxygen and nitrogen. A burst of soft x-ray emission is seen during reconnection with a new four-channel detector (SXR). There is evidence for spectral changes in the soft x-ray emission as reconnection progresses, although our single-temperature equilibrium spectral models are not able to provide adequate fits to all the SXR data. [DOI: 10.1063/1.3099603]

Conclusions

X-ray photoionization experiments are producing results

…higher X-ray fluxes (and ionization parameters) are required for direct astrophysical relevance.